

CP asymmetries in $B \rightarrow \phi K_S$ and $B \rightarrow \eta' K_S$ in MSSM

Jian-Feng Cheng^{a,b}, Chao-Shang Huang^a, and Xiao-Hong Wu^{c,d}

^a *Institute of Theoretical Physics, Academia Sinica, P. O. Box 2735, Beijing 100080, China*

^b *Institute of High Energy Physics, Academia Sinica, P. O. Box 918(4), Beijing 100039, China*

^c *Department of Physics, KAIST, Daejeon 305-701, Korea*

^d *Department of Physics, Peking University, Beijing 100871, China*

We study the $B \rightarrow \phi K_S$ and $B \rightarrow \eta' K_S$ decays in MSSM by calculating hadronic matrix elements of operators with QCD factorization approach and including neutral Higgs boson (NHB) contributions. We calculate the Wilson coefficients of operators including the new operators which are induced by NHB penguins at LO using the MIA with double insertions. We calculate the α_s order hadronic matrix elements of the new operators for $B \rightarrow \phi K_S$ and $B \rightarrow \eta' K_S$. It is shown that the recent experimental results on the time-dependent CP asymmetries in $B \rightarrow \phi K_S$ and $B \rightarrow \eta' K_S$, $S_{\phi K}$ is negative and $S_{\eta' K}$ is positive, which can not be explained in SM, can be explained in MSSM if there are flavor non-diagonal squark mass matrix elements of 2nd and 3rd generations whose size satisfies all relevant constraints from known experiments ($B \rightarrow X_S \gamma$, $B_s \rightarrow \mu^+ \mu^-$, $B \rightarrow X_s \mu^+ \mu^-$, $B \rightarrow X_s g$, ΔM_s , etc.). In particular, we find that one can explain the experimental results with a flavor non-diagonal mass insertion of chirality LL or LR or RR when α_s corrections of hadronic matrix elements of operators are included, in contrast with the claim in the literature. At the same time, the branching ratios for the two decays can also be in agreement with experimental measurements.

I. INTRODUCTION

The measurements of the time dependent CP asymmetry $S_{J/\psi K}$ in $B \rightarrow J/\psi K_S$ have established the presence of CP violation in neutral B meson decays and the measured value[1]

$$S_{J/\psi K} = \sin(2\beta(J/\psi K_S))_{\text{world-ave}} = 0.734 \pm 0.054. \quad (1)$$

is in agreement with the prediction in the standard model (SM). Recently, various measurements of CP violation in B factory experiments have attracted much interest. Among them[2, 3],

$$\begin{aligned} S_{\phi K_S} &= -0.39 \pm 0.41, & \text{2002 World - average} \\ S_{\phi K_S} &= -0.15 \pm 0.33, & \text{2003 World - average} \end{aligned} \quad (2)$$

is especially interesting since it deviates greatly from the SM expectation

$$S_{\phi K_S} = \sin(2\beta(\phi K_S)) = \sin(2\beta(J/\psi K_S)) + O(\lambda^2) \quad (3)$$

where $\lambda \simeq 0.2$ appears in Wolfenstein's parameterization of the CKM matrix. Obviously, the impact of these experimental results on the validity of CKM and SM is currently statistically limited. However, they have attracted much interest in searching for new physics [4, 5, 6, 7, 8] and it has been shown that the deviation can be understood without contradicting the smallness of the SUSY effect on $B \rightarrow J/\psi K_S$ in the minimal supersymmetric standard model (MSSM) [7, 8].

Another experimental result, which is worth to notice, is of the time dependent CP asymmetry $S_{\eta' K_S}$ in $B \rightarrow \eta' K_S$ [3, 9]

$$\begin{aligned} S_{\eta' K_S} &= 0.02 \pm 0.34 \pm 0.03 & \text{BaBar} \\ &= 0.43 \pm 0.27 \pm 0.05 & \text{Belle} \end{aligned} \quad (4)$$

which deviates sizably from the SM expectation. Although both the asymmetries $S_{\phi K}$ and $S_{\eta' K}$ are smaller than the SM value, $S_{\phi K}$ is negative and $S_{\eta' K}$ is positive. Because the quark subprocess $b \rightarrow s\bar{s}s$ contributes to both $B \rightarrow \phi K_S$ and $B \rightarrow \eta' K_S$ decays one should simultaneously explain the experimental data in a model with the same parameters. It has been done in Ref.[10] in a model-independent way in the supersymmetric (SUSY) framework. In Ref.[10] the analysis is carried out using the naive factorization to calculate hadronic matrix elements of operators and the neutral Higgs boson (NHB) contributions are not included. As we have shown in a letter[8] that both the branching ratio (Br) and CP asymmetry are significantly dependent of the α_s corrections of hadronic matrix elements and NHB contributions are important in MSSM with middle and large $\tan \beta$ (say, > 8). In the paper we shall perform

a detailed analysis of $S_{\phi K_S}$ and $S_{\eta' K}$ as well as Br in MSSM including NHB contributions and the α_s corrections of hadronic matrix elements.

We need to have new CP violation sources in addition to that of CKM matrix in order to explain the deviations of $S_{\phi K_S}$ and $S_{\eta' K}$ from SM. There are new sources of flavor and CP violation in MSSM. Besides the CKM matrix, the 6×6 squark mass matrices are generally not diagonal in flavor (generation) indices in the super-CKM basis in which superfields are rotated in such a way that the mass matrices of the quark field components of the superfields are diagonal. This rotation non-alignment in the quark and squark sectors can induce large flavor off-diagonal couplings such as the coupling of gluino to the quark and squark which belong to different generations. These couplings can be complex and consequently can induce CP violation in flavor changing neutral currents (FCNC). It is well-known that the effects of the primed counterparts of usual operators are suppressed by m_s/m_b and consequently negligible in SM because they have the opposite chirality. However, in MSSM their effects can be significant, since the flavor non-diagonal squark mass matrix elements are free parameters which are only subjective to constraints from experiments.

For the $b \rightarrow s$ transition, besides the SM contribution, there are mainly two new contributions arising from the QCD and chromomagnetic penguins and neutral Higgs boson (NHB) penguins with the gluino and squark propagated in the loop in MSSM*. The relevant Wilson coefficients at the m_W scale have been calculated by using vertex mixing method in Ref.[12]. There is the another method, "mass insertion approximation"(MIA) [13], which works in flavor diagonal gaugino couplings $\tilde{g}q\tilde{q}$ and diagonal quark mass matrices with all the flavor changes rested on the off-diagonal sfermion propagators. The MIA can be obtained in VM through Taylor expansion of nearly degenerate squark masses $m_{\tilde{q}_i}$ around the common squark mass $m_{\tilde{q}}$, $m_{\tilde{q}_i}^2 \simeq m_{\tilde{q}}^2(1 + \Delta_i)$. Thus MIA can work well for nearly degenerate squark masses and, in general, its reliability can be checked only a posteriori. However, for its simplicity, it has been widely used as a model independent analysis to find the constraints on different off-diagonal parts of squark mass matrices from experiments [14]. Therefore, we use MIA to calculate Wilson coefficients in the paper.

As it is shown that both Br and CP asymmetries depend significantly on how to calculate hadronic matrix elements of local operators[8]. Recently, two groups, Li et al. [15, 16] and BBNS [17, 18], have made significant progress in calculating hadronic matrix elements of local operators relevant to charmless two-body nonleptonic decays of B mesons in the PQCD framework. The key point to apply PQCD is to prove that the factorization, the separation of the short-distance dynamics and long-distance dynamics, can be performed for those hadronic matrix elements. It has been shown that in the heavy quark limit (i.e., $m_b \rightarrow \infty$) such a separation is indeed valid and hadronic matrix elements can be expanded in α_s such that the tree level (i.e., the α_s^0 order) is the same as that in the naive factorization and the α_s corrections can be systematically calculated[17]. Comparing with the naive factorization, to include the α_s correction decreases significantly the hadronic uncertainties. In particular, the matrix elements of the chromomagnetic-dipole operators $Q_{sg}^{(\prime)}$ have large uncertainties in the naive factorization calculation which lead to the significant uncertainty of the time dependent CP asymmetry in SUSY models[19]. The uncertainties are greatly decreased in BBNS approach[18]. In the paper we shall use BBNS's approach (QCD factorization) to calculate the hadronic matrix element of operators relevant to the decays $B \rightarrow \phi K_S, \eta' K_S$ up to the α_s order.

The experimental results, $S_{\phi K}$ is negative and $S_{\eta' K}$ is positive but smaller than 0.7, which implies that new CP violating physics affects $B \rightarrow \phi K_S$ in a dramatic way but gives $B \rightarrow \eta' K_S$ a relatively small effect, which has been thought to be problematic[20]. To solve the problem, Khalil and Kou invoke to have operators with opposite chirality because the decay constant of η' is sensitive to the chirality of the quarks and that of ϕ is independent of the chirality of the quarks, operators with opposite chirality give contributions with opposite signs to $B \rightarrow \eta' K_S$ but contributions with the same sign to $B \rightarrow \phi K_S$ [10]. In MSSM the LL (LR) and RR (RL) mass insertions give contributions to operators with opposite chirality respectively. It is shown in Ref.[10] that (1) it is possible to explain the experimental results if having both the LL and RR (or LR and RL) mass insertions simultaneously, and (2) it is impossible to explain the experimental results if having only the LL and/or LR (or RR and/or RL) insertions. The first claim is certainly valid in general. However, the second claim is of the consequence of using the naive factorization to calculate hadronic matrix elements of operators. The current-current operators contribute to $B \rightarrow \eta' K_S$ but not to $B \rightarrow \phi K_S$. Their effects are not significant in both the naive factorization approach and the QCD factorization approach. However, the α_s corrections of hadronic matrix elements of QCD penguin operators and chromomagnetic-dipole operators have significant effects and consequently make the claim (2) in Ref.[10] not valid. We show in the paper that one can explain the experimental results, $S_{\phi K}$ is negative and $S_{\eta' K}$ is positive but smaller than 0.7, with a flavor non-diagonal mass insertion of any chirality when α_s corrections of hadronic matrix elements of operators are included. We show that in the case of LL and RR mass insertions the Higgs mediated contributions to $S_{\phi K}$ alone can provide a significant deviation from the SM in some region of parameters and a possible explanation of $S_{\eta' K}$ in 1σ experimental bounds in a very small region of parameters, satisfying all the relevant experimental constraints. When including all the SUSY contributions, there are regions of parameters larger than those in the case of including only the Higgs mediated contributions in which the theoretical predictions for $S_{\phi K}$ and $S_{\eta' K}$ are in agreement with the data in 1σ experimental bounds. In the case of LR and RL insertions a satisfied explanation can also be obtained. We

* The chargino contributions have been studied in Ref.[11]

show that the branching ratio of $B \rightarrow \eta' K_S$, which in SM with the naive factorization is smaller than the measured value, can be in agreement with data due to SUSY contributions in quite a large regions of parameters.

The paper is organised as follows. In section II we give the effective Hamiltonian responsible for the $b \rightarrow s$ transition in MSSM. We give the Wilson coefficients of operators including those induced by NHBs at LO in MIA with double insertions. In Section III we present the decay amplitudes and the CP asymmetries $S_{\phi K}$ and $S_{\eta' K}$. In particular, the hadronic matrix elements of NHB induced operators to the α_s order are calculated. The Section IV is devoted to numerical results. We draw conclusions and discussions in Section V. The loop functions and some coefficients of the matrix element of the effective Hamiltonian as well as implementation of η - η' mixing are given in Appendices.

II. EFFECTIVE HAMILTONIAN

The effective Hamiltonian for $b \rightarrow s$ transition can be expressed as[8, 21]

$$\begin{aligned} \mathcal{H}_{\text{eff}} = & \frac{G_F}{\sqrt{2}} \sum_{p=u,c} V_{pb} V_{ps}^* \left(C_1 Q_1^p + C_2 Q_2^p + \sum_{i=3,\dots,16} [C_i Q_i + C'_i Q'_i] \right. \\ & \left. + C_{7\gamma} Q_{7\gamma} + C_{8g} Q_{8g} + C'_{7\gamma} Q'_{7\gamma} + C'_{8g} Q'_{8g} \right) + \text{h.c.} \end{aligned} \quad (5)$$

Here Q_i are quark and gluon operators and are given by [†]

$$\begin{aligned} Q_1^p &= (\bar{s}_\alpha p_\beta)_{V-A} (\bar{p}_\beta b_\alpha)_{V-A}, & Q_2^p &= (\bar{s}_\alpha p_\alpha)_{V-A} (\bar{p}_\beta b_\beta)_{V-A}, \\ Q_{3(5)} &= (\bar{s}_\alpha b_\alpha)_{V-A} \sum_q (\bar{q}_\beta q_\beta)_{V-(+)A}, & Q_{4(6)} &= (\bar{s}_\alpha b_\beta)_{V-A} \sum_q (\bar{q}_\beta q_\alpha)_{V-(+)A}, \\ Q_{7(9)} &= \frac{3}{2} (\bar{s}_\alpha b_\alpha)_{V-A} \sum_q e_q (\bar{q}_\beta q_\beta)_{V+(-)A}, & Q_{8(10)} &= \frac{3}{2} (\bar{s}_\alpha b_\beta)_{V-A} \sum_q e_q (\bar{q}_\beta q_\alpha)_{V+(-)A}, \\ Q_{11(13)} &= (\bar{s} b)_{S+P} \sum_q \frac{m_q}{m_b} (\bar{q} q)_{S-(+)P}, \\ Q_{12(14)} &= (\bar{s}_i b_j)_{S+P} \sum_q \frac{m_q}{m_b} (\bar{q}_j q_i)_{S-(+)P}, \\ Q_{15} &= \bar{s} \sigma^{\mu\nu} (1 + \gamma_5) b \sum_q \frac{m_q}{m_b} \bar{q} \sigma_{\mu\nu} (1 + \gamma_5) q, \\ Q_{16} &= \bar{s}_i \sigma^{\mu\nu} (1 + \gamma_5) b_j \sum_q \frac{m_q}{m_b} \bar{q}_j \sigma_{\mu\nu} (1 + \gamma_5) q_i, \\ Q_{7\gamma} &= \frac{e}{8\pi^2} m_b \bar{s}_\alpha \sigma^{\mu\nu} F_{\mu\nu} (1 + \gamma_5) b_\beta, \\ Q_{8g} &= \frac{g_s}{8\pi^2} m_b \bar{s}_\alpha \sigma^{\mu\nu} G_{\mu\nu}^a \frac{\lambda_a^{\alpha\beta}}{2} (1 + \gamma_5) b_\beta, \end{aligned} \quad (6)$$

where $(\bar{q}_1 q_2)_{V\pm A} = \bar{q}_1 \gamma^\mu (1 \pm \gamma_5) q_2$, $(\bar{q}_1 q_2)_{S\pm P} = \bar{q}_1 (1 \pm \gamma_5) q_2$ [‡], $p = u, c$, $q = u, d, s, c, b$, e_q is the electric charge number of q quark, λ_a is the color SU(3) Gell-Mann matrix, α and β are color indices, and $F_{\mu\nu}$ ($G_{\mu\nu}$) are the photon (gluon) fields strength.

The primed operators, the counterpart of the unprimed operators, are obtained by replacing the chirality in the corresponding unprimed operators with opposite ones. We calculate the SUSY contributions due to gluino box and penguin diagrams to the relevant Wilson coefficients at the m_W scale in MIA with double insertions, as investigated in Ref. [22], which are non-negligible if the mixing between left-handed and right-handed sbottoms is large and results are

$$C_3^{(\prime)} = -\frac{\alpha_s^2}{2\sqrt{2}G_F\lambda_t m_g^2} \left[\left(-\frac{1}{9}b_1(x) - \frac{5}{9}b_2(x) - \frac{1}{18}p_1(x) - \frac{1}{2}p_2(x) \right) \delta_{23}^{dLL(RR)} + \right.$$

[†] For the operators in SM we use the conventions in Ref.[18] where Q_1 and Q_2 are exchanged each other with respect to the convention in most of papers.

[‡] Strictly speaking, the sum over q in expressions of Q_i ($i=11,\dots,16$) should be separated into two parts: one is for $q=u, c$, i.e., upper type quarks, the other for $q=d, s, b$, i.e., down type quarks, because the couplings of upper type quarks to NHBs are different from those of down type quarks. In the case of large $\tan\beta$ the former is suppressed by $\tan^{-1}\beta$ with respect to the latter and consequently can be neglected. Hereafter we use, e.g., C_{11}^c to denote the Wilson coefficient of the operator $Q_{11} = (\bar{s} b)_{S+P} \frac{m_c}{m_b} (\bar{c} c)_{S-P}$.

$$\begin{aligned}
& \left(-\frac{1}{9}b'_1(x) - \frac{5}{9}b'_2(x) - \frac{1}{18}p'_1(x) - \frac{1}{2}p'_2(x)\right)\delta_{23}^{dLR(RL)}\delta_{33}^{dLR*(LR)}] \\
C_4^{(\prime)} &= -\frac{\alpha_s^2}{2\sqrt{2}G_F\lambda_t m_{\tilde{g}}^2} \left[\left(-\frac{7}{3}b_1(x) + \frac{1}{3}b_2(x) + \frac{1}{6}p_1(x) + \frac{3}{2}p_2(x)\right)\delta_{23}^{dLL(RR)} + \right. \\
& \quad \left. \left(-\frac{7}{3}b'_1(x) + \frac{1}{3}b'_2(x) + \frac{1}{6}p'_1(x) + \frac{3}{2}p'_2(x)\right)\delta_{23}^{dLR(RL)}\delta_{33}^{dLR*(LR)} \right] \\
C_5^{(\prime)} &= -\frac{\alpha_s^2}{2\sqrt{2}G_F\lambda_t m_{\tilde{g}}^2} \left[\left(\frac{10}{9}b_1(x) + \frac{1}{18}b_2(x) - \frac{1}{18}p_1(x) - \frac{1}{2}p_2(x)\right)\delta_{23}^{dLL(RR)} + \right. \\
& \quad \left. \left(\frac{10}{9}b'_1(x) + \frac{1}{18}b'_2(x) - \frac{1}{18}p'_1(x) - \frac{1}{2}p'_2(x)\right)\delta_{23}^{dLR(RL)}\delta_{33}^{dLR*(LR)} \right] \\
C_6^{(\prime)} &= -\frac{\alpha_s^2}{2\sqrt{2}G_F\lambda_t m_{\tilde{g}}^2} \left[\left(-\frac{2}{3}b_1(x) + \frac{7}{6}b_2(x) + \frac{1}{6}p_1(x) + \frac{3}{2}p_2(x)\right)\delta_{23}^{dLL(RR)} + \right. \\
& \quad \left. \left(-\frac{2}{3}b'_1(x) + \frac{7}{6}b'_2(x) + \frac{1}{6}p'_1(x) + \frac{3}{2}p'_2(x)\right)\delta_{23}^{dLR(RL)}\delta_{33}^{dLR*(LR)} \right] \\
C_{7\gamma}^{(\prime)} &= -\frac{1}{27\lambda_t} \frac{g_s^2}{g^2} \frac{m_w^2}{m_{\tilde{g}}^2} [F_2(x)\delta_{23}^{dLL(RR)} + F'_2(x)\delta_{23}^{dLR(RL)}\delta_{33}^{dLR*(LR)}] \\
& \quad - 4\frac{m_{\tilde{g}}}{m_b} F_4(x)\delta_{23}^{dLR(RL)} - 4\frac{m_{\tilde{g}}}{m_b} F'_4(x)\delta_{23}^{dLL(RR)}\delta_{33}^{dLR(LR*)}] \\
C_{8g}^{(\prime)} &= -\frac{1}{72\lambda_t} \frac{g_s^2}{g^2} \frac{m_w^2}{m_{\tilde{g}}^2} [F_{12}(x)\delta_{23}^{dLL(RR)} + F'_{12}(x)\delta_{23}^{dLR(RL)}\delta_{33}^{dLR*(LR)}] \\
& \quad - 8\frac{m_{\tilde{g}}}{m_b} F_{34}(x)\delta_{23}^{dLR(RL)} - 8\frac{m_{\tilde{g}}}{m_b} F'_{34}(x)\delta_{23}^{dLL(RR)}\delta_{33}^{dLR(LR*)}] \\
C_{11}^{(\prime)} &= \frac{e^2}{16\pi^2} \frac{m_b}{m_l} [C_{Q_1}^{(\prime)} \mp C_{Q_2}^{(\prime)}] \\
C_{13}^{(\prime)} &= \frac{e^2}{16\pi^2} \frac{m_b}{m_l} [C_{Q_1}^{(\prime)} \pm C_{Q_2}^{(\prime)}], \\
C_i^{(\prime)} &= 0, \quad i = 12, 14, 15, 16
\end{aligned} \tag{7}$$

with $C_{Q_{1,2}}^{(\prime)}$ § as

$$\begin{aligned}
C_{Q_1}^{(\prime)} &= \frac{4}{3\lambda_t} \frac{g_s^2}{g^2 s_w^2} \frac{m_b m_l}{m_H^2} \frac{c_\alpha^2 + r_s s_\alpha^2}{c_\beta^2} \frac{m_{\tilde{g}}}{m_b} f'_b(x) \delta_{23}^{dLL(RR)} \delta_{33}^{dLR(LR*)} \\
C_{Q_2}^{(\prime)} &= \mp \frac{4}{3\lambda_t} \frac{g_s^2}{g^2 s_w^2} \frac{m_b m_l}{m_A^2} (r_p + \tan^2 \beta) \frac{m_{\tilde{g}}}{m_b} f'_b(x) \delta_{23}^{dLL(RR)} \delta_{33}^{dLR(LR*)}
\end{aligned} \tag{8}$$

where $r_s = \frac{m_{H^0}^2}{m_{h^0}^2}$, $r_p = \frac{m_{A^0}^2}{m_{Z^0}^2}$, and $x = m_{\tilde{q}}^2/m_{\tilde{g}}^2$ with $m_{\tilde{q}}$ and $m_{\tilde{g}}$ being the common squark mass and gluino mass respectively. The one-loop functions in Eq. (7) are given in Appendix A. The parts of Wilson coefficients $C_i^{(\prime)}$ ($i=3, \dots, 6, 7\gamma, 8g$) which are obtained by single insertion are the same as those in Ref.[23]. Differed from the single insertion results, the LR or RL insertion also generates the QCD penguin operators when one includes the double insertions.

For the processes we are interested in this paper, the Wilson coefficients should run to the scale of $O(m_b)$. $C_1 - C_{10}$ are expanded to $O(\alpha_s)$ and NLO renormalization group equations (RGEs) should be used. However for the C_{8g} and $C_{7\gamma}$, LO results should be sufficient. The details of the running of these Wilson coefficients can be found in Ref. [21]. The one loop anomalous dimension matrices of the NHB induced operators can be divided into two distangled groups [24]

$$\gamma^{(RL)} = \begin{array}{c|cc} & Q_{11} & Q_{12} \\ \hline Q_{11} & -16 & 0 \\ Q_{12} & -6 & 2 \end{array} \tag{9}$$

§ The operator of $Q_{1,2}^{(\prime)}$ is defined as $Q_1 = \frac{e^2}{8\pi^2} [\bar{s}(1+\gamma_5)b][\bar{l}l]$, $Q'_1 = \frac{e^2}{8\pi^2} [\bar{s}(1-\gamma_5)b][\bar{l}l]$, $Q_2 = \frac{e^2}{8\pi^2} [\bar{s}(1+\gamma_5)b][\bar{l}\gamma_5 l]$, $Q'_2 = \frac{e^2}{8\pi^2} [\bar{s}(1-\gamma_5)b][\bar{l}\gamma_5 l]$

and

$$\gamma^{(RR)} = \begin{array}{c|cccc} & Q_{13} & Q_{14} & Q_{15} & Q_{16} \\ \hline Q_{13} & -16 & 0 & 1/3 & -1 \\ Q_{14} & -6 & 2 & -1/2 & -7/6 \\ Q_{15} & 16 & -48 & 16/3 & 0 \\ Q_{16} & -24 & -56 & 6 & -38/3 \end{array} \quad (10)$$

Here and hereafter the factor, $\frac{\alpha_s}{4\pi}$, is suppressed (i.e., the anomalous dimension matrix for $Q_{11,12}$ is $\frac{\alpha_s}{4\pi} \gamma^{(RL)}$, etc.). For Q'_i operators we have

$$\gamma^{(LR)} = \gamma^{(RL)} \quad \text{and} \quad \gamma^{(LL)} = \gamma^{(RR)}. \quad (11)$$

Because at present no NLO Wilson coefficients $C_i^{(n)}$, $i=11,\dots,16$, are available we use the LO running of them in the paper.

There is the mixing of the new operators induced by NHBs with the operators in SM. The leading order anomalous dimensions have been given in Refs.[25, 26]. We list those relevant to our calculations in the following. Defining

$$O_i = \frac{g^2}{16\pi^2} Q_{12+i}, \quad i = 1, 2, 3, 4, \quad (12)$$

one has

$$\gamma^{(RD)} = \begin{array}{c|cc} & Q_{7\gamma} & Q_{8g} \\ \hline O_1 & -1/3 & 1 \\ O_2 & -1 & 0 \\ O_3 & 28/3 & -4 \\ O_4 & 20/3 & -8 \end{array} \quad (13)$$

The mixing of $Q_{11,12}$ onto the QCD penguin operators is

$$\gamma^{(MQ)} = \begin{array}{c|cccc} & Q_3 & Q_4 & Q_5 & Q_6 \\ \hline O_{11} & 1/9 & -1/3 & 1/9 & -1/3 \\ O_{12} & 0 & 0 & 0 & 0 \end{array} \quad (14)$$

For the mixing among the primed operators, we have

$$\gamma^{(LD')} = \gamma^{(RD)} \quad \text{and} \quad \gamma^{(M'Q')} = \gamma^{(MQ)}. \quad (15)$$

The mixing of the new operators induced by NHBs with the operators in SM has non-negligible effects on the Wilson coefficients of the SM operators at the $O(m_b)$ scale. In particular, the Wilson coefficient of the chromo-magnetic dipole operator C_{8g} at the $O(m_b)$ scale, which has a large effect to S_{MK} ($M = \phi, \eta'$), can significantly enhance due to the mixing. To see it explicitly we concentrate on the mixing of O_i (for its definition, see Eq.(12)) onto Q_{8g} . Solving RGEs, we have

$$C_{8g}(\mu) = \sum_{c=1,\dots,4} A(\mu_0)(\eta(\mu)^{\gamma_{cc}/2\beta_0} - \eta(\mu)^{\gamma_{8g8g}/2\beta_0}) + C_{8g}(\mu_0)\eta^{\gamma_{8g8g}/2\beta_0}, \quad (16)$$

$$A(\mu_0) = \sum_{a,b=1,\dots,4} \gamma_{a1} V_{ac}^{-1} V_{cb} C_b(\mu_0) / (\gamma_{cc} - \gamma_{8g8g}) \quad (17)$$

$$\eta = \alpha_s(\mu_0) / \alpha_s(\mu), \quad (18)$$

where V and γ_{aa} are given by

$$V(\gamma^{(RR)} + 2\beta_0 I) V^{-1} = \text{diag}(\gamma_{11}, \gamma_{22}, \gamma_{33}, \gamma_{44}). \quad (19)$$

with I being the 4×4 unit matrix. Using

$$C_a(\mu_0) = C_1(\mu_0) \delta_{a1} \quad (20)$$

and Eq. (13), Eq. (16) reduces to

$$C_{8g}(\mu) = 0.68 C_{8g}(\mu_0) - 3.2 C_{13}(\mu_0), \quad (21)$$

where $C_1(\mu_0) = \frac{4\pi}{\alpha_s} C_{13}(\mu_0)$ has been used.

In our numerical calculations we neglect the contributions of EW penguin operators $Q_{7,\dots,10}$ since they are small compared with those of other operators.

III. THE DECAY AMPLITUDE AND CP ASYMMETRY

We use the BBNS approach [17, 18] to calculate the hadronic matrix elements of operators. In the approach the hadronic matrix element of an operator in the heavy quark limit can be written as

$$\langle MK_S | Q | B \rangle = \langle MK_S | Q | B \rangle_f [1 + \sum r_n \alpha_s^n], \quad (22)$$

where $\langle MK_S | Q | B \rangle_f$ indicates the naive factorization result and $M = \phi, \eta'$. The second term in the square bracket indicates higher order α_s corrections to the matrix elements [18]. We calculate the hadronic matrix elements to the α_s order in the paper. In order to see explicitly the effects of new operators in the MSSM we divide the decay amplitude into three parts. One has the same form as that in SM, the second is for primed counterparts of the SM operators, and the third is new which comes from the contributions of Higgs penguin induced operators. That is, we can write the decay amplitude for $B \rightarrow MK_S$ as

$$A(B \rightarrow MK_S) = \frac{G_F}{\sqrt{2}} A$$

$$A = A^o + A^{o'} + A^n, \quad (23)$$

$$A^{o'} = \begin{cases} A^o(C_i \rightarrow C'_i) & \text{for } B \rightarrow \phi K_S \\ A^o(C_i \rightarrow -C'_i) & \text{for } B \rightarrow \eta' K_S \end{cases} \quad (24)$$

A^o and A^n will be given in subsections.

The time-dependent CP -asymmetry S_{MK} is defined by

$$a_{MK}(t) = -C_{MK} \cos(\Delta M_{B_d^0} t) + S_{MK} \sin(\Delta M_{B_d^0} t), \quad (25)$$

where

$$C_{MK} = \frac{1 - |\lambda_{MK}|^2}{1 + |\lambda_{MK}|^2}, \quad S_{MK} = \frac{2 \text{Im} \lambda_{MK}}{1 + |\lambda_{MK}|^2}. \quad (26)$$

Here λ_{MK} is defined as

$$\lambda_{Mk} = \left(\frac{q}{p} \right)_B \frac{\mathcal{A}(\bar{B} \rightarrow MK_S)}{\mathcal{A}(B \rightarrow MK_S)}. \quad (27)$$

The ratio $(q/p)_B$ is nearly a pure phase. In SM $\lambda_{MK} = e^{i2\beta} + O(\lambda^2)$. As pointed out in Introduction, the MSSM can give a phase to the decay which we call ϕ^{SUSY} . Then we have

$$\lambda = e^{i(2\beta + \phi^{\text{SUSY}})} \frac{|\bar{\mathcal{A}}|}{|\mathcal{A}|} \Rightarrow S_{MK} = \sin(2\beta + \phi^{\text{SUSY}}) \quad (28)$$

if the ratio $\frac{|\bar{\mathcal{A}}|}{|\mathcal{A}|} = 1$. In general the ratio in the MSSM is not equal to one and consequently it has an effect on the value of S_{MK} , as can be seen from Eq.(26). Thus the presence of the phases in the squark mass matrix can alter the value of S_{MK} from the standard model prediction of $S_{MK} = \sin 2\beta_{J/\psi K} \sim 0.7$.

A. $B_d^0 \rightarrow \phi K_S$

A^o for $B_d^0 \rightarrow \phi K_S$, to the α_s order, in the heavy quark limit is given as [5, 27]

$$A^o = \langle \phi | \bar{s} \gamma_\mu s | 0 \rangle \langle K | \bar{s} \gamma^\mu b | B \rangle \times \sum_{p=u,c} V_{pb} V_{ps}^* \left[a_3 + a_4^p + a_5 - \frac{1}{2} (a_7 + a_9 + a_{10}^p) \right], \quad (29)$$

where a_i 's have been given in Refs.[5, 27] and are listed in Appendix B. The hadronic matrix element of the vector current can be parameterized as $\langle K | \bar{s} \gamma^\mu b | B \rangle = F_1^{B \rightarrow K}(q^2)(p_B^\mu + p_K^\mu) + (F_0^{B \rightarrow K}(q^2) - F_1^{B \rightarrow K}(q^2))(m_B^2 - m_K^2)q^\mu/q^2$. For the matrix element of the vector current between the vacuum and ϕ , we have $\langle \phi | \bar{s} \gamma_\mu b | 0 \rangle = m_\phi f_\phi \epsilon_\mu^\phi$.

A^n for $B_d^0 \rightarrow \phi K_S$, to the α_s order, in the heavy quark limit is given as [8]

$$A^n = A^n(C_i) + A^n(C_i \rightarrow C'_i),$$

$$A^n(C_i) = \langle \phi | \bar{s} \gamma_\mu s | 0 \rangle \langle K | \bar{s} \gamma^\mu b | B \rangle (-V_{tb} V_{ts}^*) \left[a_4^{\text{neu}} + \frac{m_s}{m_b} \left(-\frac{1}{2} a_{12} + \frac{4m_s}{m_b} a_{15} \right) \right]. \quad (30)$$

a_i 's in Eq. (30) are

$$\begin{aligned} a_4^{neu} &= \frac{C_F \alpha_s}{4\pi} \frac{P_{\phi,2}^{neu}}{N_c}, \\ a_{12} &= C_{12} + \frac{C_{11}}{N_c} \left[1 + \frac{C_F \alpha_s}{4\pi} \left(-V'_\phi - \frac{4\pi^2}{N_c} H_{K_S \phi} \right) \right], \\ a_{15} &= C_{15} + \frac{C_{16}}{N_c}, \end{aligned} \quad (31)$$

with $P_{\phi,2}^{neu}$ being

$$\begin{aligned} P_{\phi,2}^{neu} &= -\frac{1}{2} C_{11} \times \left[\frac{m_s}{m_b} \left(\frac{4}{3} \ln \frac{m_b}{\mu} - G_\phi(0) \right) + \left(\frac{4}{3} \ln \frac{m_b}{\mu} - G_\phi(1) \right) \right] \\ &+ C_{13} \left[-2 \ln \frac{m_b}{\mu} G_\phi^0 - GF_\phi(1) \right] - 4C_{15} \left[\left(-\frac{1}{2} - 2 \ln \frac{m_b}{\mu} \right) G_\phi^0 - GF_\phi(1) \right] \\ &- 8C_{16} \left[\left(\frac{m_c}{m_b} \right)^2 \left(-2 \ln \frac{m_b}{\mu} G_\phi^0 - GF_\phi(s_c) \right) \right] - 8C_{16} \left[-2 \ln \frac{m_b}{\mu} G_\phi^0 - GF_\phi(1) \right] \end{aligned} \quad (32)$$

where $s_c = m_c^2/m_b^2$ and

$$\begin{aligned} G_\phi^0 &= \int_0^1 \frac{dx}{\bar{x}} \Phi_\phi(x), \quad GF(s, x) = \int_0^1 dt \ln [s - x t \bar{t}], \\ GF_\phi(s) &= \int_0^1 dx \frac{\Phi_\phi(x)}{\bar{x}} GF(s - i\epsilon, \bar{x}) \end{aligned} \quad (33)$$

with $\bar{x} = 1 - x$ and $\Phi_\phi(x) = 6x\bar{x}$ in the asymptotic limit of the leading-twist distribution amplitude. In Eq. (31) the expressions of V' and $H_{K_S \phi}$ can be found in the Appendix B. In calculations we have set $m_{u,d} = 0$ and neglected the terms which are proportional to m_s^2/m_b^2 in Eq.(32). We have included only the leading twist contributions in Eq.(31). Here we have used the BBNS approach [17, 18] to calculate the hadronic matrix elements of operators.

B. $B_d^0 \rightarrow \eta' K_S$

A^o for $B \rightarrow \eta' K_S$, to the α_s order, in the heavy quark limit has been given in Ref.[28] as

$$\begin{aligned} A^o &= \sum_{p=u,c} V_{pb} V_{ps}^* m_B^2 A_p^o \\ A_p^o &= F^{B \rightarrow K} \left\{ f_{\eta'}^u \left[\delta_{up} a_2^p(K\eta') + 2(a_3(K\eta') - a_5(K\eta')) - \mu_{\eta'}^s (a_6^p(K\eta') - a_8^p(K\eta')) + \frac{1}{2}(-a_7(K\eta') + a_9(K\eta')) \right] \right. \\ &+ f_{\eta'}^s \left[a_3(K\eta') + a_4^p(K\eta') - a_5(K\eta') + \mu_{\eta'}^s (a_6^p(K\eta') - a_8^p(K\eta')) - \frac{1}{2}(-a_7(K\eta') + a_9(K\eta')) - \frac{1}{2}a_{10}^p(K\eta') \right] \Big\} \\ &+ F^{B \rightarrow \eta'} f_K \left[a_4^p(\eta' K) + \mu_K (a_6^p(\eta' K) - a_8^p(\eta' K)) - \frac{1}{2}a_{10}^p(\eta' K) \right], \end{aligned} \quad (34)$$

where $F^{B \rightarrow M}$ ($M=\eta', K$) is a $B \rightarrow M$ form factor calculated at $q^2 = m_K^2$ or $m_{\eta'}^2 \approx 0$. The a_i 's in Eq. (34) have been given in Ref.[28] and are listed in Appendix B.

We calculate A^n for $B \rightarrow \eta' K_S$, to the α_s order, in the heavy quark limit and the result is

$$\begin{aligned} A^n &= -V_{tb} V_{ts}^* m_B^2 [A^n(C_i) + A^n(C_i \rightarrow -C'_i)], \\ A^n(C_i) &= F^{B \rightarrow K} \left\{ f_{\eta'}^q [-\mu_{\eta'}^s (a_6^n(K\eta') - a_8^n(K\eta'))] + f_{\eta'}^s \left[a_4^n(K\eta') + \mu_{\eta'}^s (a_6^n(K\eta') - a_8^n(K\eta')) - \frac{1}{2}a_{10}^n(K\eta') \right] \right\} \\ &+ F^{B \rightarrow \eta'} f_K \left[a_4^n(\eta' K) + \mu_K (a_6^n(\eta' K) - a_8^n(\eta' K)) - \frac{1}{2}a_{10}^n(\eta' K) \right] \\ &+ F^{B \rightarrow K} \left\{ \frac{m_d}{m_b} f_{\eta'}^q \left[\frac{1}{2} \mu_{\eta'}^s \left(-a_{11} + a_{13} - \frac{1}{2}a_{14} \right) \right] + \frac{m_s}{m_b} f_{\eta'}^s \left[-\frac{1}{2}a_{12} + \frac{1}{2} \mu_{\eta'}^s \left(a_{11} - a_{13} + \frac{1}{2}a_{14} \right) \right] \right\} \\ &+ F^{B \rightarrow \eta'} \frac{m_d}{m_b} f_K \left[-\frac{1}{2}a_{12} + \mu_K \left(\frac{1}{4}a_{14} - 3a_{16} \right) \right], \end{aligned} \quad (35)$$

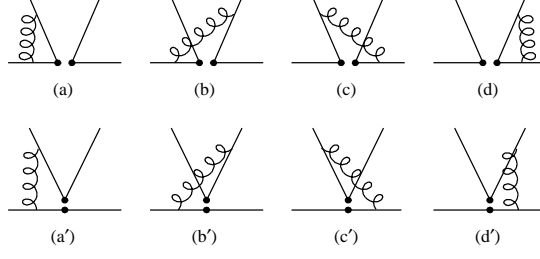


FIG. 1: vertex corrections

where decay constants $f_{\eta'}^q, f_{\eta'}^s$ are defined in Appendix C, $\mu_K = m_b R_K/2$, $\mu_{\eta'}^s = m_b R_{\eta'}^s$, and a_i^n 's and a_i 's are defined as

$$\begin{aligned}
a_4^n(M_1 M_2) &= \frac{\alpha_s}{4\pi} \frac{C_F}{N_c} P_{M_2,2}^n, & a_6^n(M_1 M_2) &= \frac{\alpha_s}{4\pi} \frac{C_F}{N_c} P_{M_2,3}^n, \\
a_8^n(M_1 M_2) &= \frac{\alpha_{\text{em}}}{9\pi} \frac{C_F}{N_c} P_{M_2,3}^{n,\text{EW}}, & a_{10}^n(M_1 M_2) &= \frac{\alpha_{\text{em}}}{9\pi} \frac{C_F}{N_c} P_{M_2,2}^{n,\text{EW}}, \\
a_{11}(M_1 M_2) &= C_{11} + \frac{C_{12}}{N_c} \\
a_{12}(M_1 M_2) &= C_{12} + \frac{C_{11}}{N_c} \left[1 + \frac{C_F \alpha_s}{4\pi} \left(-V'_{M_2} - \frac{4\pi^2}{N_c} H_{M_1 M_2} \right) \right], \\
a_{13}(M_1 M_2) &= C_{13} + \frac{C_{14}}{N_c} + C_{16} \frac{\alpha_s}{4\pi} \frac{C_F}{N_c} (-8V_{13}) \\
a_{14}(M_1 M_2) &= C_{14} + \frac{C_{13}}{N_c} + 2 \frac{\alpha_s}{4\pi} \frac{C_F}{N_c} (C_{13} V_{13} + C_{15} V_{15})
\end{aligned} \tag{36}$$

where

$$\begin{aligned}
V_{13} &= \int_0^1 du \phi_{M_2}(u) V_{S,2} + \int_0^1 du dv d\xi H_{S,3} \\
V_{15} &= \int_0^1 du \phi_{M_2}(u) V_{T,2} - 4 \int_0^1 du dv d\xi H_{S,3}
\end{aligned} \tag{37}$$

and V' , $H_{M_1 M_2}$ could be found in Appendix B. In Eqs.(36,37) $V_{S,2}$ and $V_{T,2}$ come from vertex contributions, P 's from penguin diagrams, and $H_{S,3}$ from hard-scattering contributions, which will be shown in the following. In numerical calculations we set $m_{u,d} = 0$ so that the terms which are proportional m_q ($q=u, d$) in Eq. (35) are neglected.

• Vertex Contributions

The vertex contributions come from **Fig.**(1). In the calculations of vertex corrections we need to distinguish two diagrams with different topologies showed in **Fig.**(1) when we insert different operators. In the calculation of twist-3 contributions we find the infrared divergence cancels only if we include all four diagrams for each topology and use the asymptotic form of twist-3 distribution amplitude, i.e., $\phi_p(x) = 1, \phi_\sigma(x) = 6x(1-x)$, which can be combined into $-\frac{i}{4} f_P \frac{\gamma_5 \not{k}_2 \not{k}_1}{k_2 \cdot k_1}$ [18, 29]. By a straightforward calculation, we obtain

$$\begin{aligned}
V_{S,2} &= \int_0^1 du \left\{ \left[2 + 2 \ln u - 2\bar{u} \left(\text{Li}_2 \left(1 - \frac{1}{u} \right) - \text{Li}_2 \left(1 - \frac{1}{\bar{u}} \right) \right) - 2\bar{u} (\ln u - \ln \bar{u}) \pi i \right] + \left[-11 - 6 \ln \frac{\mu^2}{m_b^2} + 3\pi i \right] \right\} \\
V_{T,2} &= \int_0^1 du \left\{ -4 \left[2 + 2 \ln u - 2\bar{u} \left(\text{Li}_2 \left(1 - \frac{1}{u} \right) - \text{Li}_2 \left(1 - \frac{1}{\bar{u}} \right) \right) - i\pi 2\bar{u} (\ln u - \ln \bar{u}) \right] + \left[32 + 24 \ln \frac{\mu^2}{m_b^2} - 12\pi i \right] \right\}
\end{aligned} \tag{38}$$



FIG. 2: The two different penguin contractions

• Penguin Contributions

In the calculations of penguin contributions we also need to consider the difference between two diagrams with different topologies showed in **Fig.(2)**. We obtain that the twist-2 parts of penguin contributions $P_{M_2,2}^n, P_{M_2,2}^{\text{EW}}$ are

$$P_{M_2,2}^n = -\frac{1}{2}C_{11} \times \left[\frac{m_s}{m_b} \left(\frac{4}{3} \ln \frac{m_b}{\mu} - G(0) \right) + \left(\frac{4}{3} \ln \frac{m_b}{\mu} - G(1) \right) \right] \\ + C_{13} \left[-2 \ln \frac{m_b}{\mu} G_{M_2}^0 - GF_{M_2}(1) \right] - 4C_{15} \left[\left(-\frac{1}{2} - 2 \ln \frac{m_b}{\mu} \right) G_{M_2}^0 - GF(1) \right] \\ - 8C_{16} \left[-2 \ln \frac{m_b}{\mu} G_{M_2}^0 - GF_{M_2}(1) \right] - 8C_{16}^c \left[\left(\frac{m_c}{m_b} \right)^2 \left(-2 \ln \frac{m_b}{\mu} G_{M_2}^0 - GF_{M_2}(s_c) \right) \right] \quad (39)$$

$$P_{M_2,2}^{n,\text{EW}} = -\frac{1}{2} \left\{ C_{12} \times \left[\frac{m_s}{m_b} \left(\frac{4}{3} \ln \frac{m_b}{\mu} - G(0) \right) + \left(\frac{4}{3} \ln \frac{m_b}{\mu} - G(1) \right) \right] \right. \\ + [C_{13} + N_c C_{14}] \left[-2 \ln \frac{m_b}{\mu} G_{M_2}^0 - GF_{M_2}(1) \right] \\ - 8[N_c C_{15} + C_{16}] \left[\left(-\frac{1}{2} - 2 \ln \frac{m_b}{\mu} \right) G_{M_2}^0 - GF_{M_2}(1) \right] \\ - 4[C_{15} + N_c C_{16}] \left(-2 \ln \frac{m_b}{\mu} G_{M_2}^0 - GF_{M_2}(1) \right) \\ \left. - 4[C_{15}^c + N_c C_{16}^c] \left[\left(\frac{m_c}{m_b} \right)^2 \left(-2 \ln \frac{m_b}{\mu} G_{M_2}^0 - GF_{M_2}(s_c) \right) \right] \right\} \quad (40)$$

where $s_c = (m_c/m_b)^2$, $G_{M_2}^0 = \int_0^1 dx \phi_{M_2}(x)/x$ and the function $GF_{M_2}(s)$ is given by

$$GF_{M_2}(s_c) = \int_0^1 dx GF(s_c, x) \frac{\phi_{M_2}(x)}{x} \quad (41)$$

Compared with twist-2 contributions, the twist-3 projection yields an additional factor of \bar{x} which has appeared in penguin contributions proportional to $C_{7\gamma}^{\text{eff}}$ and C_{8g}^{eff} . We therefore find

$$P_{M_2,3}^n = -\frac{1}{2}C_{11} \times \left[\frac{m_s}{m_b} \left(\frac{4}{3} \ln \frac{m_b}{\mu} - \widehat{G}(0) \right) + \left(\frac{4}{3} \ln \frac{m_b}{\mu} - \widehat{G}(1) \right) \right] \\ + C_{13} \left[-2 \ln \frac{m_b}{\mu} - \widehat{GF}(1) \right] - 4C_{15} \left[\left(-\frac{1}{2} - 2 \ln \frac{m_b}{\mu} \right) - \widehat{GF}(1) \right] \\ - 8C_{16} \left[-2 \ln \frac{m_b}{\mu} - \widehat{GF}(1) \right] - 8C_{16}^c \left[\left(\frac{m_c}{m_b} \right)^2 \left(-2 \ln \frac{m_b}{\mu} - \widehat{GF}(s_c) \right) \right] \quad (42)$$

$$P_{M_2,3}^{n,\text{EW}} = -\frac{1}{2} \left\{ C_{12} \times \left[\frac{m_s}{m_b} \left(\frac{4}{3} \ln \frac{m_b}{\mu} - \widehat{G}(0) \right) + \left(\frac{4}{3} \ln \frac{m_b}{\mu} - \widehat{G}(1) \right) \right] \right. \\ + [C_{13} + N_c C_{14}] \left[-2 \ln \frac{m_b}{\mu} - \widehat{GF}(1) \right] - 8[N_c C_{15} + C_{16}] \left[\left(-\frac{1}{2} - 2 \ln \frac{m_b}{\mu} \right) - \widehat{GF}(1) \right] \\ \left. - 4[C_{15} + N_c C_{16}] \left(-2 \ln \frac{m_b}{\mu} - \widehat{GF}(1) \right) - 4[C_{15}^c + N_c C_{16}^c] \left[\left(\frac{m_c}{m_b} \right)^2 \left(-2 \ln \frac{m_b}{\mu} - \widehat{GF}(s_c) \right) \right] \right\} \quad (43)$$

with

$$\widehat{GF}(s_c) = \int_0^1 dx GF(s_c, x) \phi_{M_2}(x). \quad (44)$$

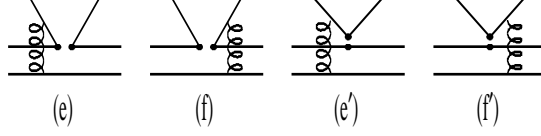


FIG. 3: hard-scattering contributions

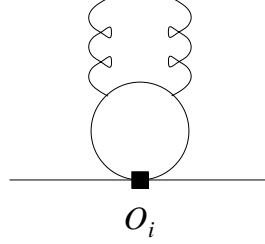


FIG. 4: Two-gluon emission from a quark loop. A second diagram with the two gluons crossed is implied.

• Hard-scattering Contributions

Hard-scattering contributions come from **Fig.(3)** which read

$$\begin{aligned}
 H_{S,3} = & \frac{1}{m_B^2 F_1^{B \rightarrow M_1}} \frac{1}{8u^2 \xi v} \left[-u \mu_{M_1} \phi_B(\xi) \frac{\phi'_{M_1 \sigma}(u)}{6} \frac{\phi'_{M_2 \sigma}(v)}{6} + 3v m_B \phi_B(\xi) \phi_{M_1}(u) \phi_{M_2 p}(v) \right. \\
 & - 3(u+v) \mu_{M_1} \phi_B(\xi) \phi_{M_1 p}(u) \phi_{M_2 p}(v) - (u-v) \mu_{M_1} \phi_B(\xi) \frac{\phi'_{M_1 \sigma}(u)}{6} \phi_{M_2 p}(v) \\
 & \left. + u \mu_{M_1} \phi_B(\xi) \phi_{M_1 p}(u) \frac{\phi'_{M_2 \sigma}(v)}{6} \right], \tag{45}
 \end{aligned}$$

where ϕ' means the derivative of ϕ . There is end-point singularity in Eq.(45) which can be treated in the way given in Appendix B.

Because η' is a flavor singlet there are three extra contributions related to the gluon content of η' . They come from: the $b \rightarrow sgg$ amplitude, spectator scattering involving two gluons, and singlet weak annihilation. As analysed in Ref.[28], the singlet weak annihilation is suppressed by at least one power of Λ_{QCD}/m_b in the heavy quark limit. So we need to calculate the contributions from the $b \rightarrow sgg$ decay and spectator scattering which have not included in the results given above. In SM the relevant calculations have been carried out and results have been given in Ref.[28]. We calculate them with insertions of new operators. In order to make the paper self-contained we also list the SM results given in Ref. [28].

Two gluon mechanism

• The $b \rightarrow sgg$ amplitude

The amplitude for $b \rightarrow sgg$ comes from **Fig. (4)**. We use the formula (16) in Ref. [28] directly. For an operator $O = (\bar{s}\Gamma_1 b)(\bar{q}\Gamma_2 q)$, where the Γ 's denote arbitrary spinor and color matrices, one has (assuming the two gluons to be in a color-singlet configuration)

$$\mathcal{A}(b \rightarrow sgg)|_{\text{Fig. 4}} = -(\bar{u}_s \Gamma_1 u_b) \langle g(q_1) g(q_2) | \text{tr}(\Gamma_2 A) | 0 \rangle, \tag{46}$$

where

$$A = \frac{\alpha_s}{4\pi N_c} \left\{ \frac{1}{12m_q} G_{\mu\nu}^A G^{A,\mu\nu} - \frac{(\not{q} - 6m_q) i\gamma_5}{48m_q^2} G_{\mu\nu}^A \tilde{G}^{A,\mu\nu} + O(1/m_q^3) \right\}. \tag{47}$$

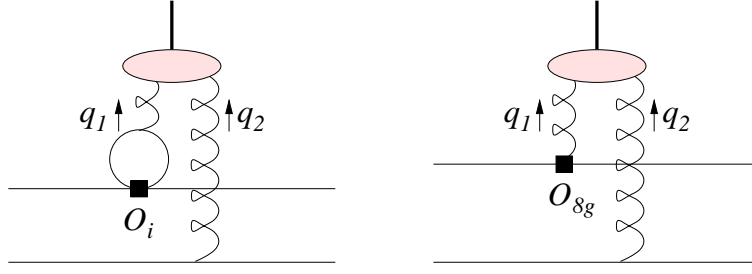


FIG. 5: Spectator-scattering contributions to the $B \rightarrow K\eta'$ decay amplitudes. The shaded blob represents the $\eta^{(\prime)} g^* g^*$ form factor.

When $\Gamma = V \pm A$, we obtain the contribution to the $\bar{B} \rightarrow \bar{K}P$ decay amplitudes

$$\mathcal{A}_p^{\text{charm}} = \frac{a_P}{12m_c^2} \langle \bar{K}(p') | \bar{s} \not{d} (1 - \gamma_5) b | \bar{B}(p) \rangle \left\{ \left(C_2 + \frac{C_1}{N_c} \right) \delta_{pc} + \left(C_3 - C_5 + \frac{C_4 - C_6}{N_c} \right) \right\}. \quad (48)$$

When $\Gamma = S \pm P$, we obtain that the decay amplitudes of $\bar{B} \rightarrow \bar{K}P$ are given as

$$\mathcal{A}_{p,n}^{\text{charm}} = \frac{a_P}{2m_c} \langle \bar{K}(p') | \bar{s} (1 + \gamma_5) b | \bar{B}(p) \rangle \left\{ \left(C_{11} + \frac{C_{12}}{N_c} \right) - \left(C_{13} + \frac{C_{14}}{N_c} \right) \right\} \quad (49)$$

• Spectator Mechanism

The **Fig.(5)** gives the spectator scattering contributions. By a straightforward calculation, we obtain the hard spectator-scattering contributions to the $B \rightarrow K\eta'$ decay amplitude using two-gluon mechanism:

$$A^{\text{spec}} = \frac{3C_F\alpha_s^2}{N_c^2} C_P f_B f_K \int_0^1 \frac{\phi_B(\xi)}{\xi} \int_0^1 \frac{dy}{y} [P_2^p (\phi_K(y) + r_\chi^K \phi_p(y)) + P_2^{\text{neu}} \phi_K(y) + r_\chi^K P_3^{\text{neu}} \phi_p(y)] \quad (50)$$

with

$$\begin{aligned} P_2^p(y) = & C_1 \left[\frac{4}{3} \ln \frac{m_b}{\mu} + \frac{2}{3} - G(s_p, \bar{y}) \right] + C_3 \left[\frac{8}{3} \ln \frac{m_b}{\mu} + \frac{4}{3} - G(0, \bar{y}) - G(1, \bar{y}) \right] \\ & + (C_4 + C_6) \left[\frac{4n_f}{3} \ln \frac{m_b}{\mu} - (n_f - 2) G(0, \bar{y}) - G(s_c, \bar{y}) - G(1, \bar{y}) \right] \\ & - \frac{1}{2} C_{11} \left[\frac{m_s}{m_b} \left(\frac{4}{3} \ln m_b \mu - G(0, \bar{y}) \right) + \left(\frac{4}{3} \ln \frac{m_b}{\mu} - G(1, \bar{y}) \right) \right] \end{aligned} \quad (51)$$

$$\begin{aligned} P_2^{\text{neu}}(y) = & -2C_{8g}^{\text{eff}} + C_{13} \left[-2 \ln \frac{m_b}{\mu} - GF(1, \bar{y}) \right] \\ & - 4C_{15} \left[-\frac{1}{2} - 2 \ln \frac{m_b}{\mu} - GF(1, \bar{y}) \right] - 8C_{16} \left[-2 \ln \frac{m_b}{\mu} - GF(1, \bar{y}) \right] \end{aligned} \quad (52)$$

$$\begin{aligned} P_3^{\text{neu}}(y) = & -2C_{8g}^{\text{eff}} + C_{13} \left[+1 - 2 \ln \frac{m_b}{\mu} - GF(1, \bar{y}) \right] \\ & - 4C_{15} \left[-\frac{3}{2} - 2 \ln \frac{m_b}{\mu} - GF(1, \bar{y}) \right] - 8C_{16} \left[-1 - 2 \ln \frac{m_b}{\mu} - GF(1, \bar{y}) \right] \end{aligned} \quad (53)$$

with $s_q = (m_q/m_b)^2$, $n_f = 5$. Obviously there is singularity arising from the end-point region in the Eq.(50) which makes us to consider the effect of k_\perp in the end-point region. After involved the k_\perp effect of spectator quark and turned to b -space, the conjugate space of k_\perp , Eq.(50) now reads

$$\begin{aligned} \mathcal{A}_p^{\text{spec}} = & \frac{3C_F\alpha_s^2}{4N_c^2} C_P f_B f_K m_B^2 \int_0^\infty b db \int_0^1 d\xi dy \mathcal{P}_B(\xi, b) \\ & \times \left\{ - [K_0(b\sqrt{-c}) - K_0(b\sqrt{a})] [P_2^p(y) (\mathcal{P}_K(y, b) + r_\chi^y \mathcal{P}_p(y, b)) + r_\chi^y P_3^{\text{neu}} \mathcal{P}_p(y, b)] \right. \\ & \left. + m_B \left[\frac{bK_1(b\sqrt{-c})}{2\sqrt{-y}} - \frac{K_0(b\sqrt{-c}) - K_0(b\sqrt{a})}{\bar{y}m_B} \right] P_2^{\text{neu}}(y) \mathcal{P}_K(y, b) \right\} \end{aligned} \quad (54)$$

where $\mathcal{P}_B(\xi, b)$, $\mathcal{P}_K(y, b)$, $\mathcal{P}_p(y, b)$ are corrected distribution amplitude including Sudakov factor [15, 16] and $K_{0(1)}$ are modified Bessel function of order 0(1). Numerically we find that the contributions from the two gluon mechanism are negligible.

IV. NUMERICAL RESULTS

A. Parameters input

In our numerical calculations the following values are needed:

- **Parameters related mixing of $\eta - \eta'$**

We use the following input [30]:

$$\begin{aligned} f_q &= f_\pi, & f_s &= \sqrt{2f_K^2 - f_\pi^2} = 1.41f_\pi, \\ h_q &= f_q m_\pi^2 = 0.0025 \text{ GeV}^3, & h_s &= f_s (2m_K^2 - m_\pi^2) = 0.086 \text{ GeV}^3, \\ \phi &= 39.3^\circ \pm 1.0^\circ. \end{aligned} \quad (55)$$

- **Lifetime, mass and decay constants**

$$\begin{aligned} \tau(B^0) &= 1.56 \times 10^{-12} \text{ s}, \quad M_B = 5.28 \text{ GeV}, \quad m_b = 4.2 \text{ GeV}, \\ m_c &= 1.3 \text{ GeV}, \quad m_s = 100 \text{ MeV}, \quad f_B = 0.190 \text{ GeV}, \quad f_K = 0.158 \text{ GeV}. \end{aligned} \quad (56)$$

- **Chiral enhancement factors**

For the chiral enhancement factors for the pseudoscalar mesons, $\mu_P = \frac{m_b R_P}{2}$, we take

$$R_{K^{\pm,0}} = R_{\pi^\pm} \simeq 1.2,$$

which are consistent with the values used in [18, 31], and

$$R_{\eta^{(\prime)}}^s = \frac{m_{\eta^{(\prime)}}^2}{m_s m_b}.$$

- **Wolfenstein parameters**

We use the Wolfenstein parameters fitted by Ciuchini et al[32]:

$$\begin{aligned} A &= 0.819 \pm 0.040, & \lambda &= 0.2237 \pm 0.0033, \\ \bar{\rho} &= \rho(1 - \lambda^2/2) = 0.224 \pm 0.038, & \rho &= 0.230 \pm 0.039, \\ \bar{\eta} &= \eta(1 - \lambda^2/2) = 0.317 \pm 0.040, & \eta &= 0.325 \pm 0.039, \\ \gamma &= (54.8 \pm 6.2)^\circ, & \sqrt{\rho^2 + \eta^2} &= 0.398 \pm 0.040. \end{aligned} \quad (57)$$

- **Form factors**

In the paper we need two form factors: $F^{B \rightarrow K}(0) = 0.34$ and $F^{B \rightarrow \eta'}$. Compared with these rather well studied form factors, the form factors for $B \rightarrow \eta^{(\prime)}$ are poorly known, which has hindered theoretical predictions for B decays involving $\eta^{(\prime)}$ very much for a long time. We adopt the following parameterization for the form factors ($P = \eta$ or η')[28]:

$$F_0^{B \rightarrow P}(0) = F_1 \frac{f_P^q}{f_\pi} + F_2 \frac{\sqrt{2}f_P^q + f_P^s}{\sqrt{3}f_\pi}, \quad (58)$$

where F_1 and F_2 both scale like $(\Lambda/m_b)^{3/2}$ in the heavy-quark limit. In our numerical analysis we set $F_1 = F_0^{B \rightarrow \pi}(0) = 0.28$ and take $F_2 = 0$.

B. Constraints from experiments

We impose two important constraints from $B \rightarrow X_s \gamma$ and $B_s \rightarrow \mu^+ \mu^-$. Considering the theoretical uncertainties, we take $2.0 \times 10^{-4} < \text{Br}(B \rightarrow X_s \gamma) < 4.5 \times 10^{-4}$, as generally analysed in literatures. Phenomenologically, $\text{Br}(B \rightarrow X_s \gamma)$ directly constrains $|C_{7\gamma}(m_b)|^2 + |C'_{7\gamma}(m_b)|^2$ at the leading order. Due to the strong enhancement factor $m_{\bar{g}}/m_b$ associated with single $\delta_{23}^{LR(RL)}$ insertion term in $C_{7\gamma}^{(\prime)}(m_b)$, $\delta_{23}^{LR(RL)}$ ($\sim 10^{-2}$) are more severely constrained than

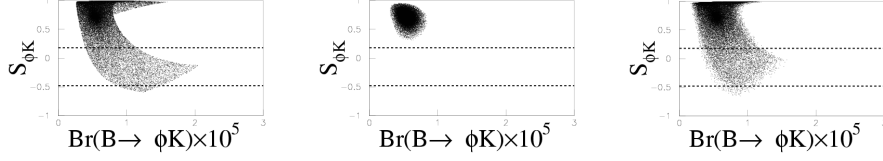


FIG. 6: The correlation between $S_{\phi K_S}$ and $\text{Br}(B \rightarrow \phi K_S)$ for the insertion of only one kind of chirality. (a) is for the LR insertion, (b) is for the LL insertion with only SM and NHB contributions included, and (c) is for the LL insertion with the all contributions included. Current 1σ bounds are shown by the dashed lines.

$\delta_{23}^{LL(RR)}$. However, if the left-right mixing of scalar bottom quark δ_{33}^{LR} is large (~ 0.5), $\delta_{23}^{LL(RR)}$ is constrained to be order of 10^{-2} since the double insertion term $\delta_{23}^{LL(RR)}\delta_{33}^{LR(LR*)}$ is also enhanced by $m_{\tilde{g}}/m_b$. The branching ratio $B_s \rightarrow \mu^+\mu^-$ in MSSM is given as

$$\text{Br}(B_s \rightarrow \mu^+\mu^-) = \frac{G_F^2 \alpha_{\text{em}}^2}{64\pi^3} m_{B_s}^3 \tau_{B_s} f_{B_s}^2 |\lambda_t|^2 \sqrt{1 - 4\hat{m}^2} [(1 - 4\hat{m}^2)|C_{Q_1}(m_b) - C'_{Q_1}(m_b)|^2 + |C_{Q_2}(m_b) - C'_{Q_2}(m_b) + 2\hat{m}(C_{10}(m_b) - C'_{10}(m_b))|^2] \quad (59)$$

where $\hat{m} = m_{\mu}/m_{B_s}$. In the middle and large $\tan\beta$ case the term proportional to $(C_{10} - C'_{10})$ in Eq. (59) can be neglected. The current experimental upper bound of $\text{Br}(B_s \rightarrow \mu^+\mu^-)$ is 2.6×10^{-6} [33]. To translate into the constraint on $C_{Q_{11,13}}$, we have

$$\sqrt{|C_{Q_{11}}(m_W) - C'_{Q_{11}}(m_W)|^2 + |C_{Q_{13}}(m_W) - C'_{Q_{13}}(m_W)|^2} \lesssim 0.1 \quad (60)$$

Because the bound constrains $|C_{Q_i} - C'_{Q_i}|$ ($i=1, 2$),[¶] we can have values of $|C_{Q_i}|$ and $|C'_{Q_i}|$ larger than those in constrained MSSM (CMSSM) with universal boundary conditions at the high scale and scenarios of the extended minimal flavor violation in MSSM [7] in which $|C'_{Q_i}|$ is much smaller than $|C_{Q_i}|$. At the same time we require that predicted Br of $B \rightarrow X_s \mu^+\mu^-$ falls within 1σ experimental bounds.

We also impose the current experimental lower bound $\Delta M_s > 14.4 \text{ ps}^{-1}$ [36] and experimental upper bound $\text{Br}(B \rightarrow X_s g) < 9\%$ [37]. Because $\delta_{23}^{LR(RL)}$ is constrained to be order of 10^{-2} by $\text{Br}(B \rightarrow X_s \gamma)$, their contribution to ΔM_s is small. The dominant contribution to ΔM_s comes from $\delta_{23}^{LL(RR)}$ insertion with both constructive and destructive effects compared with the SM contribution, where the too large destructive effect is ruled out, because SM prediction is only slightly above the present experiment lower bound.

As pointed out in section II, due to the gluino-sbottom loop diagram contribution and the mixing of NHB induced operators onto the chromomagnetic dipole operator, the Wilson coefficients $C_{8g}^{(\prime)}$ can be large, which might lead to a too large Br of $B \rightarrow X_s g$. So we need to impose the constraint from experimental upper bound $\text{Br}(B \rightarrow X_s g) < 9\%$. A numerical analysis for $C_{8g}'=0$ has been performed in Ref.[26]. We carry out a similar analysis by setting both C_{8g} and C_{8g}' non-zero.

C. Numerical results for $B \rightarrow \phi K_S$

In numerical analysis we fix $m_{\tilde{g}} = m_{\tilde{q}} = 400 \text{ GeV}$ and $\tan\beta = 30$. We vary the NHB masses in the ranges of $91 \text{ GeV} \leq m_h \leq 135 \text{ GeV}$, $91 \text{ GeV} \leq m_H \leq 200 \text{ GeV}$ with $m_h < m_H$ and $200 \text{ GeV} \leq m_A \leq 250 \text{ GeV}$ for the fixed mixing angle $\alpha = 0.6, \pi/2$ of the CP even NHBs and scan δ_{23}^{dAB} in the range $|\delta_{23}^{dAB}| \leq 0.05$ for $A=B$ and 0.01 for $A \neq B$ ($A = L, R$).

Numerical results for $B \rightarrow \phi K_S$ are shown in **Figs. 6, 7** where the correlation between $S_{\phi K_S}$ and $\text{Br}(B \rightarrow \phi K_S)$ is plotted. **Fig. 6** is for the insertion of only one kind of chirality. 6(a), 6(b) and 6(c) correspond to the LR insertion, the LL insertion with only NHB and SM contributions included, and the LL insertion with the all contributions included, respectively. We find that for the LR insertion (**Fig. 6(a)**) and the LL insertion (**Fig. 6(c)**) there are regions of parameters where $S_{\phi K_S}$ falls in 1σ experimental bounds and Br is smaller than 1.6×10^{-5} . In the case of the LL insertion with only NHB and SM contributions included (**Fig. 6(b)**) $S_{\phi K_S} \geq 0.3$ because $C_i' = 0$, $i=11, \dots, 16$

[¶] $C_{Q_{1,2}}^{(\prime)}$ are the Wilson coefficients of the operators $Q_{1,2}^{(\prime)}$ which are Higgs penguin induced in leptonic and semileptonic B decays and their definition can be found in Ref. [34]. By substituting the quark-Higgs vertex for the lepton-Higgs vertex it is straightforward to obtain Wilson coefficients relevant to hadronic B decays.

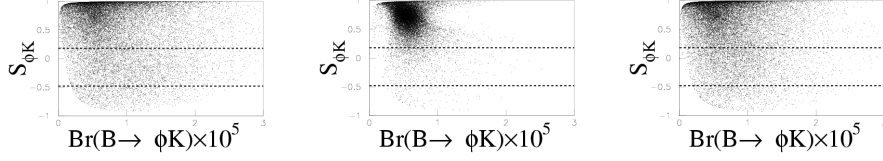


FIG. 7: The correlation between $S_{\phi K_S}$ and $\text{Br}(B \rightarrow \phi K_S)$. (a) is for the LR and RL insertions, (b) is for the LL and RR insertions with only SM and NHB contributions included, and (c) is for the LL and RR insertions with the all contributions included. Current 1σ bounds are shown by the dashed lines.

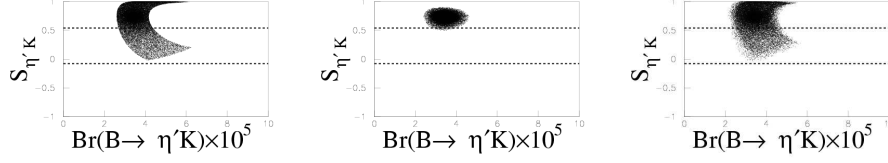


FIG. 8: The correlation between $S_{\eta' K_S}$ and $\text{Br}(B \rightarrow \eta' K_S)$ for the insertion of only one kind of chirality. (a) is for the LR insertion, (b) is for the LL insertion with only SM and NHB contributions included, and (c) is for the LL insertion with the all contributions included. Current 1σ bounds are shown by the dashed lines.

and consequently C_i , $i=11, \dots, 16$ can not be as large as in the case with both the LL and RR insertions due to the constraint from $B_s \rightarrow \mu^+ \mu^-$. The similar result is obtained for only a RL insertion or a RR insertion. In **Fig. 7**, 7(a), 7(b), and 7(c) correspond to the LR and RL insertions, the LL and RR insertions with only NHB and SM contributions included, and the LL and RR insertions with the all contributions included, respectively. We find that there are regions of parameters where $S_{\phi K_S}$ falls in 1σ experimental bounds and Br is smaller than 1.6×10^{-5} in all three cases. The difference among the three cases is that the size of the regions is different: the smallest ones are for the LL and RR insertions with only NHB and SM contributions included, and the biggest ones for the LL and RR insertions with the all contributions included, as expected. In the cases of the LL and RR insertions and the LR and RL insertions $S_{\phi K_S}$ can reach -0.9 or so. Comparing 6(a) 6(c) with 7(a) 7(c), one can see that the case with both the LR and RL insertions (both the LL and RR insertions) has parameter regions with negative $S_{\phi K_S}$ larger than those in the case with the LR (LL) insertion.

D. Numerical results for $B \rightarrow \eta' K_S$

Input parameters used in this subsection are the same as those in last subsection. Numerical results for $B \rightarrow \eta' K_S$ are shown in **Figs. 8, 9** where the correlation between $S_{\eta' K_S}$ and $\text{Br}(B \rightarrow \eta' K_S)$ is plotted. The **Fig. 8** is for the insertion of only one kind of chirality. 8(a), 8(b), and 8(c) correspond to the LR insertion, the LL insertion with only NHB and SM contributions included, and the LL insertion with the all contributions included, respectively. In all three cases $S_{\eta' K_S} \geq 0$ and in the case of the LL insertion with only NHB and SM contributions included the minimal value of $S_{\eta' K_S}$ is 0.5 . The similar result is obtained for only a RL insertion or a RR insertion. In **Fig. 9**, 9(a), 9(b), and 9(c) correspond to the LR and RL insertions, the LL and RR insertions with only NHB and SM contributions included, and the LL and RR insertions with the all contributions included, respectively. We find that there are regions of parameters where $S_{\eta' K_S}$ falls in 1σ experimental bounds and Br is larger than 2.7×10^{-5} and smaller than 11×10^{-5} in the first and third cases. For the first case, i.e., the case of the LR and RL insertions, there is most of

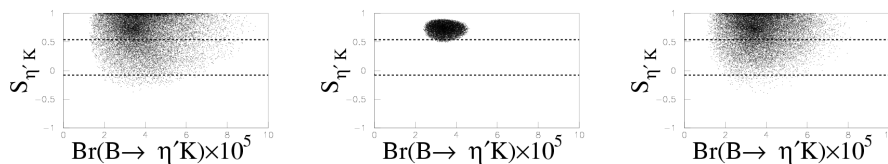


FIG. 9: The correlation between $S_{\eta' K_S}$ and $\text{Br}(B \rightarrow \eta' K_S)$. (a) is for the LR and RL insertions, (b) is for the LL and RR insertions with only SM and NHB contributions included, and (c) is for the LL and RR insertions with the all contributions included. Current 1σ bounds are shown by the dashed lines.

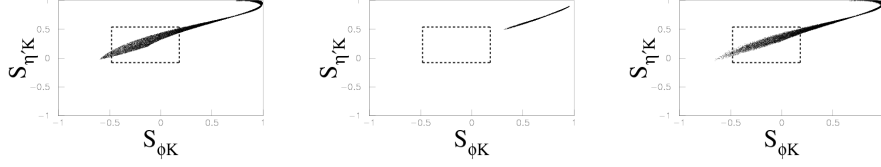


FIG. 10: The correlation between $S_{\eta'K_S}$ and $S_{\phi K_S}$ for the insertion of only one kind of chirality. (a) is for the LR insertion, (b) is for the LL insertion with only SM and NHB contributions included, and (c) is for the LL insertion with the all contributions included. Current 1σ bounds are shown by the dashed lines.

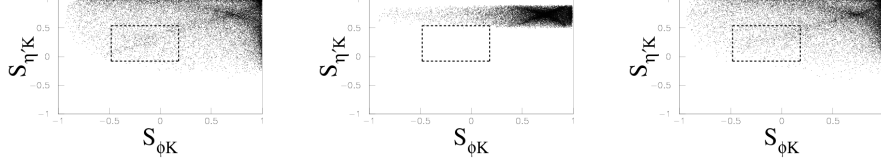


FIG. 11: The correlation between $S_{\eta'K_S}$ and $S_{\phi K_S}$. (a) is for the LR and RL insertions, (b) is for the LL and RR insertions with only SM and NHB contributions included, and (c) is for the LL and RR insertions with the all contributions included. Current 1σ bounds are shown by the dashed lines.

region of parameters where $S_{\eta'K_S}$ is positive. In the third case, i.e., the case of the LL and RR insertions with the all contributions included, the region which corresponds to positive $S_{\eta'K_S}$ increases. For the second case, i.e., the case of the LL and RR insertions with only NHB and SM contributions included, $S_{\eta'K_S} \geq 0.5$ in all regions of parameters, in contrast to the cases of the LR and RL insertions and the LL and RR insertions with the all contributions included. The reason is that the new contributions come mainly from the combination $C_{13}(m_W) - C'_{13}(m_W)$ which is constrained by $B_s \rightarrow \mu^+ \mu^-$. It is the same reason that make **Fig. 9(b)** similar to **Fig. 8(b)**. We would like to note that our results on $\text{Br}(B \rightarrow \eta' K_S)$ can agree with the experimental measurement [35]

$$\text{Br}(B \rightarrow \eta' K) = (5.8^{+1.4}_{-1.3}) \times 10^{-5} \quad (61)$$

Indeed, it has been shown that the data can be explained within theoretical uncertainties in SM without introducing any new mechanism[28].

In order to show explicitly there is the region of parameters in which $S_{\eta'K_S}$ is positive and $S_{\phi K_S}$ is negative for a set of values of parameters we plot the correlation between $S_{\phi K_S}$ and $S_{\eta'K_S}$ in **Figs. 10, 11**. The **Fig. 10** is devoted to the case with an insertion of only one kind of chirality. **Fig. 10(a)** is for the LR insertion, **Fig. 10(b)** and **Fig. 10(c)** are for only NHB and SM contributions included and the all contributions included, respectively, with the LL insertion. One can see from **Fig. 10(a)** that there is the region in which $S_{\eta'K_S}$ is positive and $S_{\phi K_S}$ is negative and their minimal values are 0 and -0.6 , respectively. **Fig. 10(b)** shows that with only the LL insertion there is no region in which $S_{\eta'K_S}$ is positive and $S_{\phi K_S}$ is negative if one includes only NHB and SM contributions. The reason is that $C'_{11,13}(m_W) = 0$ without a RR insertion (see, eg. (7)) so that the $\text{Br}(B_s \rightarrow \mu^+ \mu^-)$ upper bound limits the size of $C'_{11,13}$, which leads to $S_{\phi K_S} \geq 0.3$, as shown in **Fig. 6(b)**. When switching on all SUSY contributions among which the contribution coming from the chromo-magnetic dipole operator is dominant because its Wilson coefficient can be large due to including the double insertions (see, Eq. (7)), there is the region in which $S_{\eta'K_S}$ is positive and $S_{\phi K_S}$ is negative and their minimal values are 0 and -0.7 , respectively, as shown in **Fig. 10(c)**. We would like to point out that our result in the case with only an LL insertion is different from that in Ref.[10] because we include the α_s corrections of hadronic matrix elements and the effects of NHB induced operators. We have also calculated the correlation between $S_{\phi K_S}$ and $S_{\eta'K_S}$ in the case with only an RL insertion and an RR insertion respectively. In the case with only an RL insertion, although there is the region in which $S_{\eta'K_S}$ is positive and $S_{\phi K_S}$ is negative but there is no region in which both $S_{\eta'K_S}$ and $S_{\phi K_S}$ are in agreement with data in the 1σ bound. In the case with only an RR insertion, there are some points in the parameter space for which both $S_{\eta'K_S}$ and $S_{\phi K_S}$ are in agreement with data in the 1σ bound.

Fig. 11 is for (a) the LR and RL insertions, (b) only NHB and SM contributions included and (c) the all contributions included with the LL and RR insertions. We can see from the figure that the region exists for all three cases. For the case of the LR and RL insertions, there is a small region in which both $S_{\eta'K_S}$ and $S_{\phi K_S}$ are negative. For the case of the LL and RR insertions with only NHB and SM contributions included, the region of parameters in which $S_{\eta'K_S}$ is positive and $S_{\phi K_S}$ is negative is smaller than that in the case of the LR and RL insertions and there is no region in which both $S_{\eta'K_S}$ and $S_{\phi K_S}$ are negative. There is almost no region in which $S_{\eta'K_S}$ is smaller than -0.5 for the case of the LL and RR insertions with the all contributions included and also for the case of LR and RL insertions.

The numerical results are obtained for $m_{\tilde{g}} = m_{\tilde{q}} = 400$ GeV. For smaller gluino and squark masses, the Wilson coefficient $C_{8g}^{(\prime)}$ becomes larger, which could make the effect on S_{MK} and Br larger. However, indeed the effect is limited due to the constraint from $B \rightarrow X_s g$. For fixed $m_{\tilde{g}}$, the Wilson coefficient $C_{8g}^{(\prime)}$ is not sensitive to the variation of the mass of squark in the range about from 100 GeV to 1.5 TeV. Therefore, the numerical results are not sensitive to the squark mass and would have a sizable change when the gluino mass decreases. For the very big gluino and squark masses (say, several TeV), SUSY effects drop, i.e., one reaches the decoupling limit.

V. CONCLUSIONS AND DISCUSSIONS

In summary we have calculated the Wilson coefficients at LO for the new operators which are induced by NHB penguins using the MIA with double insertions in the MSSM. We have calculated the α_s order hadronic matrix elements of the new operators for $B \rightarrow \phi K_S$ and $B \rightarrow \eta' K_S$ in the QCD factorization approach. Using the Wilson coefficients and hadronic matrix elements obtained, we have calculated the time-dependent CP asymmetries $S_{\phi K}$ and $S_{\eta' K}$ and branching ratios for the decays $B \rightarrow \phi K_S$ and $B \rightarrow \eta' K_S$. It is shown that in the reasonable region of parameters where the constraints from $B_s - \bar{B}_s$ mixing, $\Gamma(b \rightarrow s\gamma)$, $\Gamma(b \rightarrow sg)$, $\Gamma(b \rightarrow s\mu^+\mu^-)$, $B \rightarrow \mu^+\mu^-$ are satisfied, the branching ratio of the decay for $B \rightarrow \phi K_S$ can be smaller than 1.6×10^{-5} , and $S_{\phi K_s}$ can be negative. In some regions of parameters $S_{\phi K_s}$ can be as low as -0.9 . The branching ratio and the time dependent CP asymmetry of the decay for $B \rightarrow \eta' K_S$ can agree with experiments within 1σ deviation in quite a large region of parameters. In particular, our result in the case with only an LL insertion or an RR insertion is different from that in Ref.[10] because we include the α_s corrections of hadronic matrix elements of operators and the effects of NHB induced operators.

It is necessary to make a theoretical prediction in SM as precision as we can in order to give a firm ground for finding new physics. For the purpose, we calculate the twist-3 and weak annihilation contributions in SM using the method in Ref. [38] by which there is no any phenomenological parameter introduced. The numerical results show that the annihilation contributions to Br are negligible, the twist-3 contributions to Br are also very small, smaller than one percent, and both the annihilation and twist-3 contributions to the time-dependent CP asymmetry are negligible. The conclusion remains in MSSM and we have neglected the annihilation contributions in numerical calculations.

In conclusion, we have shown that the recent experimental measurements on the time-dependent CP asymmetry in $B \rightarrow \phi K_S$ and $B \rightarrow \eta' K_S$, which can not be explained in SM, can be explained in MSSM if there are flavor non-diagonal squark mass matrix elements of second and third generations whose size satisfies all relevant constraints from known experiments ($B \rightarrow X_S \gamma$, $B_s \rightarrow \mu^+\mu^-$, $B \rightarrow X_s \mu^+\mu^-$, $B \rightarrow X_s g$, ΔM_s , etc.). Therefore, if the present experimental results remain in the future, it will signal the significant breakdown of the standard model and that MSSM is a possible candidate of new physics.

Acknowledgement

The work was supported in part by the National Nature Science Foundation of China. XHW is supported by KOSEF Sundo Grant R02-2003-000-10085-0 and the China Postdoctoral Science Foundation. One of the authors(JFC) are grateful to Professor C.-D. Lü and Y.-D. Yang for their helpful comments and discussions.

Note added

When completing the paper we received the reference [40]. In Ref. [40] the new bound of $Br(B_s \rightarrow \mu^+\mu^-)$ is given as

$$Br(B_s \rightarrow \mu^+\mu^-) < 5.8 \times 10^{-7} \quad \text{at } 90\% \text{ confidence level.}$$

The new bound would give a more stringent constraint on the contributions of NHBs. We have carried out preliminary calculations. The preliminary results show that it is still possible that NHB contributions to S_{MK} ($M = \phi, \eta'$) alone can make a sizable even significant deviation from the SM. In other words, the qualitative conclusion in the paper is still valid if using the new bound.

References

-
- [1] B. Aubert et al, BABAR Collaboration, Phys. Rev. Lett. **89** (2002) 201802; K. Abe et al, Belle Collaboration, arXiv:hep-ex/0308036.
- [2] Aubert et al. (BABAR Collaboration), hep-ex/0207070; T. Augshev, talk given at ICHEP 2002 (Belle Collaboration), BELLE-CONF-0232; K. Abe et al., BELLE-CONF-0201 hep-ex/0207098.
- [3] The Belle Collaboration, K. Abe et al, hep-ex/0308035(BELLE-CONF-0344); the talk given by T. Browder at LP2003, http://conferences.fnal.gov/lp2003/program/S5/browder_s05_ungarbled.pdf.
- [4] M. B. Causse, hep-ph/0207070; G. Hiller, Phys. Rev. **D66** (2002) 071502; A. Datta, Phys. Rev. **D66**(2002) 071702; M. Raidal, Phys. Rev. Lett. **89**(2002) 231803; K. Agashe and C.D. Carone, hep-ph/0304229; B. Dutta, C.S. Kim, S. Oh, Phys. Rev. Lett. **90** (2003) 011801; J.-P. Lee, K.Y. Lee, hep-ph/0209290; Y.-L. Wu, Y.-F. Zhou, hep-ph/0403252.
- [5] C.-S. Huang and S.-H. Zhu, Phys. Rev. **D68** (2003) 114020[arXiv:hep-ph/0307354].
- [6] M. Ciuchini, L. Silvestrini, Phys. Rev. Lett. **89**(2002) 231802; L. Silvestrini, hep-ph/0210031(talk contributed at ICHEP02); S. Khalil, E. Kou, Phys. Rev. **D67** (2003) 055009; R. Harnik, D.T. Larson, H. Murayama, A. Pierce, hep-ph/0212180; A. Kundu and T. Mitra, hep-ph/0302123; R. Arnowitt, B. Dutta and B. Hu, Phys. Rev. **D68** (2003) 075008; J. Hisano, Y. Shimizu, hep-ph/0308255; C. Dariescu, M. A. Dariescu, N.G. Deshpande and D. K. Ghosh, hep-ph/0308305; Y. Wang, hep-ph/0309290; V. Barger, C.-W. Chiang, P. Langacker, H.-S. Lee, hep-ph/0310073; S. Mishima, A. I. Sanda, hep-ph/0311068; N. G. Deshpande, D. K. Ghosh, hep-ph/0311332; B. Dutta, C. S. Kim, S. Oh, G. Zhu, hep-ph/0312389; C.H. Chen, C.Q. Geng, hep-ph/0403188.
- [7] G.L. Kane et al., hep-ph/0212092, Phys. Rev. Lett. **90** (2003) 141803.
- [8] J.-F. Cheng, C.-S. Huang and X.-H. Wu, Phys. Lett. **B 585** (2004) 287 [arXiv:hep-ph/0306086].
- [9] B. Aubert, et al., BABAR Collaboration, Phys. Rev. Lett. **91** (2003) 161801.
- [10] S. Khalil, E. Kou, Phys. Rev. Lett. **91** (2003) 241602.
- [11] S. Baek, Phys. Rev. **D67** (2003) 096004; D. Chakraverty, E. Gabrielli, K. Huitu, and S. Khalil, Phys. Rev. **D68** (2003) 095004.
- [12] C.-S. Huang and X.-H. Wu, Nucl. Phys. **B657**(2003) 304.
- [13] L. J. Hall, V. A. Kostelecky, S. Raby, Nucl. Phys. **B267** (1986) 415.
- [14] For a review, see: F. Gabbiani, E. Gabrielli, A. Masiero, L. Silvestrini, Nucl. Phys. **B477** (1996) 321.
- [15] H.-n. Li and H. Yu, Phys. Rev. Lett. **74** (1995) 4388; H.-n. Li and T. Yeh, Phys. Rev. **D56** (1997) 1615.
- [16] Y. Y. Keum, H.-n. Li and A. I. Sanda, Phys. Lett. **B504** (2001) 6; Phys. Rev. **D63** (2001) 054008.
- [17] M. Beneke et al., Phys. Rev. Lett. **83**(1999) 1914; Nucl. Phys. **B591**(2000) 313.
- [18] M. Beneke et al., Nucl. Phys. **B606**(2001) 245.
- [19] R. Harnik, D.T. Larson, H. Murayama, A. Pierce, hep-ph/0212180.
- [20] Y. Nir, Nucl. Phys. Proc. Suppl. **117** (2003) 111.
- [21] G. Buchalla, A. J. Buras and M. E. Lautenbacher, Rev. Mod. Phys. **68**(1996) 1125 [arXiv:hep-ph/9512380].
- [22] L. Everett, G. L. Kane, S. Rigolin, L. -T. Wang, and T. T. Wang, JHEP 0201 (2002) 022.
- [23] S.W. Baek, J.H. Jang, P. Ko and J.H. Park, Nucl. Phys. **B609**(2001) 442 .
- [24] J.A. Bagger, K.T. Matchev and R.J. Zhang, Phys. Lett. **B412**(1997) 77; M. Ciuchini et al., Nucl. Phys. **B523**(1998) 501; C.-S. Huang and Q.-S. Yan, hep-ph/9906493; A.J. Buras, M. Misiak and J. Urban, Nucl.Phys. **B586** (2000) 397.
- [25] F. Borzumati, C. Greub, T. Hurth and D. Wyler, Phys. Rev. **D62**(2000) 075005 .
- [26] G. Hiller, F. Krüger, hep-ph/0310219.
- [27] X.-G. He, J.P. Ma and C.-Y. Wu, Phys. Rev. **D63** (2001) 094004 ; H.-Y. Cheng and K.C. Yang, Phys. Rev. **D64**(2001) 074004.
- [28] M. Beneke and M. Neubert, Nucl. Phys. **B651** (2003) 225.
- [29] B.V. Geshkenbein and M.V. Terentev, Phys. Lett. **117**(1982) 243 .
- [30] R. Kaiser and H. Leutwyler, Proceedings of Workshop on Nonperturbative Methods in Quantum Field Theory, Adelaide, 1998 [hep-ph/9806336]; R. Kaiser and H. Leutwyler, Eur. Phys. J. C **17** (2000) 623 [hep-ph/0007101].
- [31] Hai-Yang Cheng, Yong-Yeon Keum and Kwei-Chou Yang, Phys.Rev.**D65** (2002) 094023.
- [32] M. Ciuchini *et al*, J. High Energy Phys. **07**(2001) 13.
- [33] CDF Collaboration, F. Abe et al., Phys. Rev. **D57**(1998) 3811.
- [34] Y.-B. Dai, C.-S. Huang and H.-W. Huang, Phys. Lett. **B390**(1997) 257; C.-S. Huang and Q.-S. Yan, Phys. Lett. **B442**(1998) 209 ; C.-S. Huang, W. Liao, and Q.-S. Yan, Phys. Rev. **D59**(1999) 011701.
- [35] K. Hagiwara et al., Phys. Rev. **D66** (2002) 010001.
- [36] A. Stocchi, Nucl. Phys. Proc. Suppl. **117**(2003) 145 [arXiv:hep-ph/0211245].
- [37] A. Kagan, hep-ph/9806266; T.E. Coan et al. (CLEO Collaboration), Phys. Rev. Lett. **80** (1998) 1150.
- [38] J.-F. Cheng and C.-S. Huang, Phys. Lett. **B554**(2003) 155 . In the paper the constraint from $B \rightarrow \mu^+ \mu^-$ is not imposed.
- [39] R. Harnik, D. T. Larson, H. Murayama, A. Pierce, arXiv:hep-ph/0212180.
- [40] D. Acosta et al. (CDF Collaboration), hep-ex/0403032.
- [41] T. Feldmann, P. Kroll and B. Stech, Phys. Rev. D **58**(1998) 114006 [hep-ph/9802409]; T. Feldmann, Int. J. Mod. Phys. A **15**(2000) 159 [hep-ph/9907491].

Appendix A Loop functions

In this Appendix, we present the one-loop function of Wilson coefficients in this work.

$$\begin{aligned}
b_{1,2}(x) &= x \frac{\partial B_{1,2}(x, y)}{\partial x} \Big|_{y \rightarrow x} \\
p_{1,2}(x) &= x \frac{\partial C_{1,2}(x, y)}{\partial x} \Big|_{y \rightarrow x} \\
F_{2,12,4,34}(x) &= x \frac{\partial f_{2,12,4,34}(x)}{\partial x} \\
b'_{1,2}(x) &= \frac{x^2}{2} \frac{\partial^2 B_{1,2}(x, y)}{\partial x^2} \Big|_{y \rightarrow x} \\
p'_{1,2}(x) &= \frac{x^2}{2} \frac{\partial^2 C_{1,2}(x, y)}{\partial x^2} \Big|_{y \rightarrow x} \\
F'_{2,12,4,34}(x) &= \frac{x^2}{2} \frac{\partial^2 f_{2,12,4,34}(x)}{\partial x^2} \\
f'_b(x) &= \frac{x^2}{2} \frac{\partial^2 f_{b0}(x)}{\partial x^2}
\end{aligned} \tag{62}$$

with

$$f_{12}(x) = 9f_1(x) + f_2(x), \quad f_{34}(x) = 9f_3(x) + f_4(x)/2$$

where $B_{1,2}(x, y)$ and $C_{1,2}(x, y)$ are defined in Ref. [39] and $f_{1,2,3,4,b0}$ in Ref. [12].

Appendix B Coefficients a_i

We shall give the explicit expressions of coefficients a_i of the matrix element of the effective Hamiltonian in SM [18, 28] which are not given in the content. For the integral which contains end-point singularity, we give a corrected one by including transverse momentum effects of partons and the Sudakov factor. The coefficients a_i can generally be divided into two parts $a_i(M_1 M_2) = a_{i,I}(M_1 M_2) + a_{i,II}(M_1 M_2)$:

$$\begin{aligned}
a_{1,I} &= C_1 + \frac{C_2}{N_c} \left[1 + \frac{C_F \alpha_s}{4\pi} V_{M_2} \right], & a_{1,II} &= \frac{C_2}{N_c} \frac{C_F \pi \alpha_s}{N_c} H, \\
a_{2,I} &= C_2 + \frac{C_1}{N_c} \left[1 + \frac{C_F \alpha_s}{4\pi} V_{M_2} \right], & a_{2,II} &= \frac{C_1}{N_c} \frac{C_F \pi \alpha_s}{N_c} H, \\
a_{3,I} &= C_3 + \frac{C_4}{N_c} \left[1 + \frac{C_F \alpha_s}{4\pi} V_{M_2} \right], & a_{3,II} &= \frac{C_4}{N_c} \frac{C_F \pi \alpha_s}{N_c} H, \\
a_{4,I}^p &= C_4 + \frac{C_3}{N_c} \left[1 + \frac{C_F \alpha_s}{4\pi} V_{M_2} \right] + \frac{C_F \alpha_s}{4\pi} \frac{P_{M_2,2}^p}{N_c}, & a_{4,II} &= \frac{C_3}{N_c} \frac{C_F \pi \alpha_s}{N_c} H, \\
a_{5,I} &= C_5 + \frac{C_6}{N_c} \left[1 + \frac{C_F \alpha_s}{4\pi} (-V'_{M_2}) \right], & a_{5,II} &= \frac{C_6}{N_c} \frac{C_F \pi \alpha_s}{N_c} (-H), \\
a_{6,I}^p &= C_6 + \frac{C_5}{N_c} \left(1 - 6 \cdot \frac{C_F \alpha_s}{4\pi} \right) + \frac{C_F \alpha_s}{4\pi} \frac{P_{M_2,3}^p}{N_c}, & a_{6,II} &= 0, \\
a_{7,I} &= C_7 + \frac{C_8}{N_c} \left[1 + \frac{C_F \alpha_s}{4\pi} (-V'_{M_2}) \right], & a_{7,II} &= \frac{C_8}{N_c} \frac{C_F \pi \alpha_s}{N_c} (-H), \\
a_{8,I}^p &= C_8 + \frac{C_7}{N_c} \left(1 - 6 \cdot \frac{C_F \alpha_s}{4\pi} \right) + \frac{\alpha}{9\pi} \frac{P_{M_2,3}^{p,EW}}{N_c}, & a_{8,II} &= 0, \\
a_{9,I} &= C_9 + \frac{C_{10}}{N_c} \left[1 + \frac{C_F \alpha_s}{4\pi} V_{M_2} \right], & a_{9,II} &= \frac{C_{10}}{N_c} \frac{C_F \pi \alpha_s}{N_c} H, \\
a_{10,I}^p &= C_{10} + \frac{C_9}{N_c} \left[1 + \frac{C_F \alpha_s}{4\pi} V_{M_2} \right] + \frac{\alpha}{9\pi} \frac{P_{M_2,2}^{p,EW}}{N_c}, & a_{10,II} &= \frac{C_9}{N_c} \frac{C_F \pi \alpha_s}{N_c} H
\end{aligned}$$

where M_2 means the "emission" meson, which is ϕ in the process $B \rightarrow K\phi$ and is η' or K in the process $B \rightarrow \eta'K$. The vertex contributions in Eq. (63) are given as following:

$$\begin{aligned} V_{M_2} &= 12 \ln \frac{m_b}{\mu} - 18 + \int_0^1 dx g(x) \Phi_{M_2}(x), \\ V'_{M_2} &= 12 \ln \frac{m_b}{\mu} - 6 + \int_0^1 dx g(1-x) \Phi_{M_2}(x), \\ g(x) &= 3 \left(\frac{1-2x}{1-x} \ln x - i\pi \right) \\ &\quad + \left[2 \text{Li}_2(x) - \ln^2 x + \frac{2 \ln x}{1-x} - (3 + 2i\pi) \ln x - (x \leftrightarrow 1-x) \right], \end{aligned} \quad (63)$$

The constants 18 and 6 are specific to the NDR scheme. Next, the penguin contributions are

$$\begin{aligned} P_{M_2,2}^p &= C_1 \left[\frac{4}{3} \ln \frac{m_b}{\mu} + \frac{2}{3} - G_{M_2}(s_p) \right] + C_3 \left[\frac{8}{3} \ln \frac{m_b}{\mu} + \frac{4}{3} - G_{M_2}(0) - G_{M_2}(1) \right] \\ &\quad + (C_4 + C_6) \left[\frac{4n_f}{3} \ln \frac{m_b}{\mu} - (n_f - 2)G_{M_2}(0) - G_{M_2}(s_c) - G_{M_2}(1) \right] \\ &\quad - 2C_{8g}^{\text{eff}} \int_0^1 \frac{dx}{1-x} \Phi_{M_2}(x), \\ P_{M_2,2}^{p,\text{EW}} &= (C_1 + N_c C_2) \left[\frac{4}{3} \ln \frac{m_b}{\mu} + \frac{2}{3} - G_{M_2}(s_p) \right] - 3 C_{7\gamma}^{\text{eff}} \int_0^1 \frac{dx}{1-x} \Phi_{M_2}(x), \end{aligned} \quad (64)$$

where $n_f = 5$ is the number of light quark flavours, and $s_u = 0$, $s_c = (m_c/m_b)^2$ are mass ratios involved in the evaluation of the penguin diagrams. The small contributions from electroweak penguin operators are neglected in $P_{M_2,2}^p$ within our approximations. Similar comments apply to (67) below. The function $G_{M_2}(s)$ is given by

$$G_{M_2}(s) = \int_0^1 dx G(s - i\epsilon, 1-x) \Phi_{M_2}(x), \quad (65)$$

$$G(s, x) = -4 \int_0^1 du u(1-u) \ln[s - u(1-u)x]. \quad (66)$$

Compared with the twist-2 terms, the twist-3 terms do not have factor $1-x$, which is cancelled in the calculation. We therefore find

$$\begin{aligned} P_{M_2,3}^p &= C_1 \left[\frac{4}{3} \ln \frac{m_b}{\mu} + \frac{2}{3} - \hat{G}_{M_2}(s_p) \right] + C_3 \left[\frac{8}{3} \ln \frac{m_b}{\mu} + \frac{4}{3} - \hat{G}_{M_2}(0) - \hat{G}_{M_2}(1) \right] \\ &\quad + (C_4 + C_6) \left[\frac{4n_f}{3} \ln \frac{m_b}{\mu} - (n_f - 2)\hat{G}_{M_2}(0) - \hat{G}_{M_2}(s_c) - \hat{G}_{M_2}(1) \right] - 2C_{8g}^{\text{eff}}, \\ P_{M_2,3}^{p,\text{EW}} &= (C_1 + N_c C_2) \left[\frac{4}{3} \ln \frac{m_b}{\mu} + \frac{2}{3} - \hat{G}_{M_2}(s_p) \right] - 3 C_{7\gamma}^{\text{eff}}, \end{aligned} \quad (67)$$

with

$$\hat{G}_{M_2}(s) = \int_0^1 dx G(s - i\epsilon, 1-x) \Phi_p^{M_2}(x). \quad (68)$$

The hard-scattering contributions $H_{M_1 M_2}$ are defined as following:

$$H_{M_1 \phi} \propto \int d\xi du dv \left[\frac{\phi_B(\xi)}{\xi} \frac{\phi_{M_1}(u)}{u} \frac{\phi_{M_2}(v)}{v} + \frac{2\mu_{M_1}}{m_B} \frac{\phi_B(\xi)}{\xi} \frac{\frac{\phi_{\sigma}(u)}{6}}{u^2} \frac{\phi_{M_2}(v)}{v} \right]. \quad (69)$$

We assume

$$\Phi_B(x) = N_B x^2 (1-x)^2 \exp \left[-\frac{m_B^2 x^2}{2\omega_B^2} \right] \quad (70)$$

with normalization factor N_B satisfying $\int_0^1 dx \Phi_B(x) = 1$, which is the popular used form in literature. Fitting various B decay data, ω_B is determined to be 0.4 GeV [16]. With the Sudakov effects to cancel end-point singularity, Eq.(69)

turns into

$$\begin{aligned}
H_{M_1\phi} &\propto \int d\xi du dv d^2\mathbf{k}_\perp d^2\mathbf{k}_{1\perp} d^2\mathbf{k}_{2\perp} \\
&\times \left[\frac{-um_B^4 \phi_B(\xi) \phi_{M_1}(u) \phi_{M_2}(v)}{[\xi um_B^2 + (\mathbf{k}_\perp - \mathbf{k}_{1\perp})^2][-uvm_B^2 + (\mathbf{k}_\perp - \mathbf{k}_{1\perp} + \mathbf{k}_{2\perp})^2]} \right. \\
&\quad \left. + \frac{2\mu_{M_1} m_B^5 uv \phi_B(\xi) \frac{\phi_\sigma(u)}{6} \phi_{M_2}(v)}{[\xi um_B^2 + (\mathbf{k}_\perp - \mathbf{k}_{1\perp})^2][-uvm_B^2 + (\mathbf{k}_\perp - \mathbf{k}_{1\perp} + \mathbf{k}_{2\perp})^2]} \right]. \tag{71}
\end{aligned}$$

Calculating the upper integral in b space, we obtain the hard spectator scattering contribution

$$\begin{aligned}
H_{M_1\phi} &= \frac{4\pi^2}{N_c} \frac{f_{M_1} f_B}{F_+^{B \rightarrow M_1} (m_\phi^2) m_B^2} \int dx dy dz \int b db b_2 db_2 \mathcal{P}_B(z, b) \mathcal{P}_{M_2}(x, b_2) \\
&\times \left\{ -um_B^4 \mathcal{P}_{M_1}(y, b) K_0(vb_2) \times [\theta(b_2 - b) I_0(ub) K_0(ub_2) + \theta(b - b_2) I_0(ub_2) K_0(ub)] \right. \\
&\quad \left. + 2uv \mu_{M_1} m_B^5 \frac{\mathcal{P}_\sigma(y, b)}{6} \frac{b_2}{2v} K_{-1}(vb_2) \times [\theta(b_2 - b) I_0(ub) K_0(ub_2) + \theta(b - b_2) I_0(ub_2) K_0(ub)] \right\} \tag{72}
\end{aligned}$$

where K_i , I_i are modified Bessel functions of order i and \mathcal{P}_B , \mathcal{P}_{M_1} , \mathcal{P}_{M_2} are B , M_1 , M_2 corrected meson amplitudes with the exponentials S_B , S_{M_2} and S_{M_1} respectively [15, 16]

Appendix C. Implementation of η - η' mixing

Though in the calculation of weak decay amplitudes we only consider the case with an η' meson in the final state, we have to include the effect from η - η' mixing. In the following discussions we use the FKS scheme to describe the mixing between η - η' [28, 41]. The matrix elements of local operators evaluated between the vacuum and $\eta^{(\prime)}$, of the flavor-diagonal axial-vector and pseudoscalar current densities, read

$$\begin{aligned}
\langle P(q) | \bar{q} \gamma^\mu \gamma_5 q | 0 \rangle &= -\frac{i}{\sqrt{2}} f_P^q q^\mu, & 2m_q \langle P(q) | \bar{q} \gamma_5 q | 0 \rangle &= -\frac{i}{\sqrt{2}} h_P^q, \\
\langle P(q) | \bar{s} \gamma^\mu \gamma_5 s | 0 \rangle &= -i f_P^s q^\mu, & 2m_s \langle P(q) | \bar{s} \gamma_5 s | 0 \rangle &= -i h_P^s,
\end{aligned} \tag{73}$$

where $q = u$ or d . We assume exact isospin symmetry and identify $m_q \equiv \frac{1}{2}(m_u + m_d)$. We also need the anomaly matrix elements

$$\langle P(q) | \frac{\alpha_s}{4\pi} G_{\mu\nu}^A \tilde{G}^{A,\mu\nu} | 0 \rangle = a_P, \tag{74}$$

where we use the convention

$$\tilde{G}^{A,\mu\nu} = -\frac{1}{2} \epsilon^{\mu\nu\alpha\beta} G_{\alpha\beta}^A \quad (\epsilon^{0123} = -1) \tag{75}$$

for the dual field-strength tensor. In all cases $P = \eta$ or η' denotes the physical pseudoscalar meson state.

The Eq.(73) and Eq.(74) including ten non-perturbative parameters f_P^i , h_P^i , and a_P , which however are not all independent, connect by

$$\partial_\mu (\bar{q} \gamma^\mu \gamma_5 q) = 2im_q \bar{q} \gamma_5 q - \frac{\alpha_s}{4\pi} G_{\mu\nu}^A \tilde{G}^{A,\mu\nu} \tag{76}$$

(and similarly with q replaced by s) yields four relations between the various parameters, which can be summarised as

$$a_P = \frac{h_P^q - f_P^q m_P^2}{\sqrt{2}} = h_P^s - f_P^s m_P^2. \tag{77}$$

which leaves us with six independent parameters now.

The physical states are related to the flavor states in the FKS scheme by The

$$\begin{pmatrix} |\eta\rangle \\ |\eta'\rangle \end{pmatrix} = \begin{pmatrix} \cos \phi & -\sin \phi \\ \sin \phi & \cos \phi \end{pmatrix} \begin{pmatrix} |\eta_q\rangle \\ |\eta_s\rangle \end{pmatrix}, \tag{78}$$

where $|\eta_q\rangle = (|u\bar{u}\rangle + |d\bar{d}\rangle)/\sqrt{2}$ and $|\eta_s\rangle = |s\bar{s}\rangle$, then the same mixing angle applies to the decay constants f_P^i and h_P^i with the normalization given by (73). We can re-define the decay constants in terms of $f_{s,q}$ and a mixing angle ϕ as

$$\begin{aligned} f_\eta^q &= f_q \cos \phi, & f_\eta^s &= -f_s \sin \phi, \\ f_{\eta'}^q &= f_q \sin \phi, & f_{\eta'}^s &= f_s \cos \phi, \end{aligned} \quad (79)$$

and an analogous set of equations for the h_P^i . Inserting these results into (77) allows us to express all ten non-perturbative parameters in terms of the decay constants f_q, f_s and the mixing angle ϕ . We obtain

$$h_q = f_q (m_\eta^2 \cos^2 \phi + m_{\eta'}^2 \sin^2 \phi) - \sqrt{2} f_s (m_{\eta'}^2 - m_\eta^2) \sin \phi \cos \phi, \quad (80)$$

$$h_s = f_s (m_{\eta'}^2 \cos^2 \phi + m_\eta^2 \sin^2 \phi) - \frac{f_q}{\sqrt{2}} (m_{\eta'}^2 - m_\eta^2) \sin \phi \cos \phi, \quad (81)$$

and

$$a_\eta = -\frac{1}{\sqrt{2}} (f_q m_\eta^2 - h_q) \cos \phi = -\frac{m_{\eta'}^2 - m_\eta^2}{\sqrt{2}} \sin \phi \cos \phi (-f_q \sin \phi + \sqrt{2} f_s \cos \phi), \quad (82)$$

$$a_{\eta'} = -\frac{1}{\sqrt{2}} (f_q m_{\eta'}^2 - h_q) \sin \phi = -\frac{m_{\eta'}^2 - m_\eta^2}{\sqrt{2}} \sin \phi \cos \phi (f_q \cos \phi + \sqrt{2} f_s \sin \phi). \quad (83)$$